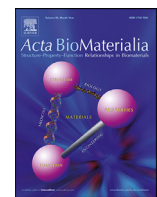




Contents lists available at ScienceDirect



Full length article

Hyaluronan improves photoreceptor differentiation and maturation in human retinal organoids

Kotoe Kawai^{a,c,1}, Margaret T. Ho^{a,b,1}, Yui Ueno^{a,c,d}, Dhana Abdo^{a,b}, Chang Xue^{a,b}, Hidenori Nonaka^c, Hiroyuki Nishida^c, Yoichi Honma^c, Valerie A. Wallace^{e,f}, Molly S. Shoichet^{a,b,d,g,*}

^a Terrence Donnelly Centre for Cellular and Biomolecular Research, University of Toronto, Canada^b Institute of Biomedical Engineering, University of Toronto, Canada^c Regenerative Medicine Research and Planning Division, Rohto Pharmaceutical Co., Ltd., 6-5-4 Kunimidai, Kizugawa, Kyoto 619-0216, Japan^d Department of Chemical Engineering and Applied Chemistry, University of Toronto, Canada^e Department of Laboratory Medicine and Pathobiology, University of Toronto, Canada^f Department of Ophthalmology and Vision Sciences, University of Toronto, Canada^g Department of Chemistry, University of Toronto, Canada

ARTICLE INFO

Article history:

Received 24 November 2023

Revised 24 April 2024

Accepted 1 May 2024

Available online xxx

Keywords:

Human retinal organoid

Hyaluronan

Photoreceptor development

Outer segment

ABSTRACT

Human stem cell-derived organoids enable both disease modeling and serve as a source of cells for transplantation. Human retinal organoids are particularly important as a source of human photoreceptors; however, the long differentiation period required and lack of vascularization in the organoid often results in a necrotic core and death of inner retinal cells before photoreceptors are fully mature. Manipulating the *in vitro* environment of differentiating retinal organoids through the incorporation of extracellular matrix components could influence retinal development. We investigated the addition of hyaluronan (HA), a component of the interphotoreceptor matrix, as an additive to promote long-term organoid survival and enhance retinal maturation. HA treatment had a significant reduction in the proportion of proliferating (Ki67+) cells and increase in the proportion of photoreceptors (CRX+), suggesting that HA accelerated photoreceptor commitment *in vitro*. HA significantly upregulated genes specific to photoreceptor maturation and outer segment development. Interestingly, prolonged HA-treatment significantly decreased the length of the brush border layer compared to those in control retinal organoids, where the photoreceptor outer segments reside; however, HA-treated organoids also had more mature outer segments with organized discs structures, as revealed by transmission electron microscopy. The brush border layer length was inversely proportional to the molar mass and viscosity of the hyaluronan added. This is the first study to investigate the role of exogenous HA, viscosity, and polymer molar mass on photoreceptor maturation, emphasizing the importance of material properties on organoid culture.

Statement of Significance

Retinal organoids are a powerful tool to study retinal development *in vitro*, though like many other organoid systems, can be highly variable. In this work, Shoichet and colleagues investigated the use of hyaluronan (HA), a native component of the interphotoreceptor matrix, to improve photoreceptor maturation in developing human retinal organoids. HA promoted human photoreceptor differentiation leading to mature outer segments with disc formation and more uniform and healthy retinal organoids. These

* Corresponding authors at: The Donnelly Centre for Cellular & Biomolecular Research, 160 College Street, (Room 530), Toronto, Ontario, Canada.

E-mail address: molly.shoichet@utoronto.ca (M.S. Shoichet).¹ Authors contributed equally to this work.

findings highlight the importance of adding components native to the developing retina to generate more physiologically relevant photoreceptors for cell therapy and *in vitro* models to drive drug discovery and uncover novel disease mechanisms.

© 2024 The Authors. Published by Elsevier Ltd on behalf of Acta Materialia Inc.
This is an open access article under the CC BY-NC-ND license
(<http://creativecommons.org/licenses/by-nc-nd/4.0/>)

1. Introduction

Stem cell-derived retinal organoids permit the study of human retinal development *in vitro* [1,2]. Under the right conditions, human pluripotent stem cells self-organize into three-dimensional laminated tissues that can give rise to all seven cell types of the retina [3]. Over the past decade, there have been several protocols for generating retinal organoids from human pluripotent stem cells, using either the serum-free floating embryoid body (SFEBq) method [2–7] or the 2D/3D protocol that bypasses the need to generate embryoid bodies [8,9]. These methods have revolutionized the field of vision science, paving the way for advances in cell transplantation [8,10–12] and enabling more predictive drug screening [13–15] and disease modelling [16–24].

Notwithstanding these advances, there are several limitations of retinal organoids. Photoreceptors are highly dependent on the retinal pigment epithelium (RPE) for nutrient transport, secretion of neurotrophic factors, isomerization of retinal, which is required for phototransduction, and renewal of photoreceptor outer segments [25]. Not all retinal organoids have RPE, and typically they are found in small ectopic patches. Due to the long differentiation period required to mature photoreceptor cells and the lack of vascularization in current protocols, the static culture conditions often result in the death of the inner cells of the organoid, such as retinal ganglion, bipolar, horizontal, and amacrine cells, which limit the study of synaptic development and the relevance of disease modeling *in vitro*. To improve retinal differentiation and maintenance, many studies have explored the addition of antioxidants, decellularized extracellular matrix (ECM), or use of microfluidic technologies [26–28]. While additives have improved retinal differentiation and photoreceptor development, it is difficult to attribute these effects to specific proteins in bulk decellularized ECM extracts. We wondered if the addition of the extracellular (and interphotoreceptor) matrix component, hyaluronan, would overcome some of the challenges associated with long-term human retinal organoid culture.

Hyaluronan (HA) is a polymer chain composed of repeating units of the disaccharide β -(1→4)-*d*-glucuronic acid β -(1→3)-*N*-acetyl-*d*-glucosamine. HA is required in early neural development when the anterior neural plate folds into the neural tube [29], is secreted by the RPE, and is a large component of the interphotoreceptor matrix, enveloping the photoreceptor inner and outer segments [25,30–32]. HA is produced by hyaluronan synthases (HAS proteins) and can be found in both the inner plexiform and the photoreceptor cells of the developing retina [33]. In addition to matrix support through its mechanical and viscoelastic properties, HA is also involved in CD44 signaling and upregulation of the mTOR pathway [34]. Interestingly, HA promoted the survival of primary mouse photoreceptors cultured *in vitro* [34] and transplanted mouse retinal stem cell-derived photoreceptors *in vivo* [35]. When CD44 signalling was perturbed in human stem-cell derived retinal organoids through the use of blocking antibodies, photoreceptor development was impacted [36]. Thus, HA is a compelling and relevant ECM component to test for enhanced human retinal organoid differentiation.

Mitrousis et al. first demonstrated that HA-based hydrogels had a pro-survival effect on primary rod photoreceptors *in vitro*. The

stiffness of the hydrogel, which was changed by increasing the concentration of HA in the gel (varying from 0.8 % to 2.75 %), did not have a significant effect on the viability of photoreceptors [34]. Based on this previously established work, we chose to use one consistent concentration of HA and investigated the effect of molar mass on both primary mouse photoreceptors and developing retinal organoids.

We investigated the effect of adding hyaluronan to the culture media of differentiating retinal organoids on retinal cell viability, cell proliferation, and photoreceptor maturation. The role of molar mass on cell viability was first examined in primary mouse photoreceptors and then human retinal organoids. HA restricted retinal organoid size compared to age-matched controls, and to investigate this further, we explored changes in cell proliferation, preservation of laminated layers, and expression of photoreceptor genes and proteins. Transmission electron microscopy (TEM) was employed to examine changes in photoreceptor outer segment development at the ultrastructural level. We demonstrate that HA enhances photoreceptor differentiation and disc packing in photoreceptor outer segments in 3D human retinal organoids, which would not be possible to study in a 2D setting. With improved human retinal organoid culture, cell therapies, drug screening platforms, more faithful models of disease will be enhanced.

2. Materials & methods

2.1. Preparation of sterile hyaluronan

Sodium hyaluronate (LifeCore Biomedical) ranging from 20 to 1000 kDa in molar mass, was sterile-filtered through a 0.22 μ m filter, lyophilized, and stored at -20 °C until use (**Supplemental Table 1**). For cell culture treatments, polymers were dissolved in the appropriate media.

2.2. Isolation of mouse retinal dissociates

Animal work was approved by the Animal Care Committee at the University of Toronto according to the Canadian Council on Animal Care. Retinas were isolated from postnatal day 3–5 C57BL/6J mice and dissociated into a single cell suspension using a papain dissociation kit, according to the manufacturer's instructions (Worthington Industries, Columbus, OH, USA). To isolate live photoreceptors, retinal dissociates were stained with a mouse CD73-PE antibody for 30 min on ice (Biolegend, San Diego, California, USA). Antibodies are listed in **Supplemental Table 2**. DAPI (Cell Signaling Technology, Danvers, MA, USA) was added to the sorting buffer (2 % BSA in PBS with 100 U/ml of DNase I) as a viability marker. Photoreceptors were sorted on the BD FACS Melody into cold collection buffer (10 % BSA in PBS). Unsorted retinal dissociates and sorted photoreceptors were seeded in 96-well plates at 2×10^5 cells/well in retinal explant medium (**Supplemental Table 3**). For analysis of cell viability, live and dead cells were stained with calcein AM and ethidium homodimer (Biotium, Fremont, California, USA) respectively and imaged on confocal. Cells were quantified semi-automatically using Imaris (version 8.3.1).

For quantification of live mouse photoreceptors using flow cytometry, cultures were dissociated using TrypLE for 15 min, and

pelleted at $300 \times g$ for 5 min. The samples were stained with CD73-PE or CD73-APC for 30 min on ice and eFluor780 fixable viability dye for 10 min. The cells were washed and fixed in 4 % PFA for 10 min at room temperature. Prior to acquisition, fluorescent counting beads (Thermofisher Scientific, Waltham, MA, USA) were added to each sample. Data was acquired on the BD LSR Fortessa X-20. Single cells were gated by forward height (FSC-H) by forward width scatter (FSC-W) followed by side height and side width scatter (SSC-H vs SSC-W). Live photoreceptors were then gated by CD73+;eFluor780- events and normalized to the number of collected fluorescent counting beads.

2.3. Retinal organoid differentiation

Retinal organoids were generated from H9 and CRX-GFP H9 (gift from Majlinda Lako's Lab) stem cell lines. Human pluripotent stem cells were maintained on Geltrex (Thermofisher Scientific, Mississauga, ON, Canada) coated plates in either mTESR+ (STEMCELL Technologies, Vancouver, ON, Canada) or Essential 8 (E8) medium (Thermofisher Scientific, Waltham, MA, USA) and passaged using ReLeSR (STEMCELL Technologies, Vancouver, ON, Canada). To initiate retinal organoid differentiation, the stem cells were cultured in E8 medium until 90–100 % confluence. The cells were then fed with Essential 6 medium for 2 days and then transitioned into N-2 supplement-rich medium for 3 weeks. Upon the appearance of laminated neuroretinal tissues, the confluent 2D cultures were scraped and maintained in suspension culture in polyHEMA coated plates for the remainder of the differentiation protocol. Media was switched to retinal initiation medium (RIM), supplemented with B27 (without vitamin A) for 2 weeks. The organoids transitioned to retinal maturation media (RMM) from week 6 to week 9, which was supplemented with taurine, FBS, and retinoic acid. Full media compositions are listed in **Supplemental Table 4**.

HA treatment was initiated at 14 weeks of differentiation and continued up until differentiation week 26, with half media changes replenished twice weekly. To reduce any variability in the amount of secreted HA from the RPE, organoids with minimal RPE were selected. Organoids with large patches of RPE were manually dissected prior to use in experiments. Organoids were harvested between week 16, week 20, and week 26 for gene and protein expression analysis. For additional studies on brush border length, HA treatment was started at week 28 until week 32 (for ultrastructural analysis) or from week 32–34 (for viscosity studies). Retinal organoids from the CRX-GFP H9 cell line were used for flow cytometry and qRT-PCR. Retinal organoids differentiated from H9 cells were used for brush border measurements, TEM, and immunohistochemistry.

2.4. Immunohistochemistry

Retinal organoids were washed in PBS before fixation in 4 % PFA for 15 min at room temperature. The fixed samples were washed 3 times (5 min each) in PBS and equilibrated in 30 % sucrose overnight. Organoids were embedded in optimal cutting temperature (OCT), snap frozen in chilled isopentane, and stored at -80°C until sectioning. Retinal organoids were sectioned onto SuperFrost Plus slides and stored at -20°C . Cryosections were permeabilized with 0.3 % Triton-X for 15 min at room temperature (RT). The slides were blocked with 10 % donkey serum, 0.1 % Triton-X for 1 h at RT. Primary antibodies were diluted in 1 % donkey serum + 0.1 % Triton-X overnight at 4°C . On the following day, the sections were washed with PBS + 0.1 % Triton-X (PBST) three times and then incubated secondary antibodies for 1 h at RT. Subsequently, the sections were washed with PBST three times and counterstained with Hoechst. Slides were mounted with ProLongTM

Gold Antifade Mountant (Thermofisher Scientific, Waltham, MA, USA). Antibodies are listed in **Supplemental Table 2**.

2.5. Imaging

Confocal images were acquired on either an Olympus FV1000 or Zeiss LSM 880. Images used for comparison or quantification were taken with identical parameters. For quantifying whole organoid images, slides were scanned using the Zeiss AxioScan slide scanner or tile scanned on the LSM 880.

2.6. Quantitative reverse transcription PCR (qRT-PCR)

A minimum of 10–15 retinal organoids were pooled together and washed in PBS. The samples were lysed with RA1 buffer (Macherey-Nagel, Düren, Nordrhein-Westfalen, Germany) and immediately stored at -80°C or proceeded with RNA extraction according to the manufacturer's instructions. Synthesis of cDNA was performed using the Superscript VILO synthesis cDNA kit (Thermofisher Scientific, Waltham, MA, USA). The cDNA was amplified using Sso Advanced SYBR Green master mix (Bio-Rad Laboratories, Hercules, CA, USA) and run on the QuantStudio 6 Flex Real Time-PCR System for 40 cycles. Primer sequences are listed in **Supplemental Table 5** and **Supplemental Table 6**. GAPDH was used as a housekeeping gene and ΔCt values were normalized to undifferentiated stem cells ($\Delta\Delta\text{Ct}$).

2.7. Flow cytometry

Retinal organoids (7–10 organoids pooled per biological replicate) were dissociated into a single cell suspension using papain and incubated at 37°C for 40–50 min. The papain was neutralized in final maturation media and the cells were pelleted in a 96 well V-bottom plate by centrifuging at $300 \times g$ for 5 min. The cells were washed in FACS buffer (0.5 % BSA in PBS and 0.05 % sodium azide). Samples were counted and viability was checked by trypan blue. The samples were stained with UV-Zombie Fixable Viability dye (1:800 in PBS) for 10 min, RT. For staining nuclear markers (Ki67), the cells were fixed and permeabilized using the eBioscience Foxp3 Fixation/Permeabilization kit. For staining of intracellular markers (recoverin), samples were fixed in 4 % PFA for 30 min on ice. After washing with PBS, the samples were resuspended in 0.1 % saponin in FACS buffer for 15 min, RT to permeabilize the cells. Primary antibody staining (diluted in 0.1 % saponin) was performed for 30 min, RT. The samples were stained with secondary antibodies (diluted in 0.1 % saponin) for 30 min, RT. Cells were washed twice and resuspended in FACS buffer.

Data was acquired on the BD LSR Fortessa. Cells were first gated by FSC-A and SSC-A, then doublet discrimination was performed by forward height (FSC-H) vs forward width scatter (FSC-W), followed by side height (SSC-H) vs side width scatter (SSC-W). Dead cells were gated out by the fixable UV-zombie stain and proliferating or CRX-GFP+ photoreceptors were gated on viable cells. Data was analyzed on FlowJoTM v10.7 software (BD Biosciences, San Jose, CA, USA).

2.8. Transmission electron microscopy (TEM)

Organoids were prepared using the standard methods [37] for the Embed 812 resin kit (Electron Microscopy Sciences, EMS). Briefly, organoids were fixed with 4 % PFA, 1 % glutaraldehyde in 0.1 M phosphate buffer, pH 7.2 for 1 h, RT and then overnight at 4°C . Organoids were washed 3× with 0.1 M phosphate buffer, pH 7.2 for 15 min each at RT. The samples were secondary fixed with 1 % OsO₄ in 0.1 M phosphate buffer for 1 h RT in the dark. The samples were washed again 3× with 0.1 M phosphate buffer, pH 7.2 for

10 min at RT. The samples were dehydrated in a gradient ethanol series: 30 % ethanol for 15 min, 50 % ethanol for 20 min, 70 % ethanol for 30 min, 90 % ethanol for 45 min, and 100 % ethanol for 60 min. The samples were infiltrated with the Embed 812 resin kit (EMS) diluted with propylene oxide: 100 % propylene oxide for 20 min, 33 % (v/v) Embed 812 resin mixture in propylene oxide for 2 h, 67 % (v/v) Embed 812 resin mixture in propylene oxide for 3 h, 100 % Embed 812 resin mixture overnight, fresh 100 % Embed 812 resin mixture for 2 h. After infiltration organoids in resin were put in BEEM capsules and cured at 65 °C for 48 h.

The resin blocks were sectioned with a Reichert Ultracut E microtome (Leica) to 80 nm thickness and collected on 300 mesh copper grids (EMS). The sections were counter stained using saturated 5 % uranyl acetate (EMS) for 10 min followed by Reynold's lead citrate (EMS) for 10 min. Prepared grids were placed on a filter paper mat in labelled Petri dishes and store in a desiccator until imaging.

The sections were imaged and examined in a Talos L120C transmission electron microscope (Thermo Scientific) at an accelerating voltage of 120KV. Organoids were examined at magnifications from 2600 \times to 57,000 \times resulting in a field of view of 22.4 μ m down to 1.02 μ m, and a pixel size of 5.46 nm down to 249 pm.

2.9. Rheology

HA was sterile-filtered and lyophilized as described above. The polymers were then dissolved overnight in DMEM/F12 at a concentration of 10 mg/ml. The polymer properties were measured using a Discovery HR-2 hybrid rheometer using a 20 mm, 1° cone plate. A flow ramp was performed on each sample at 37 °C, measuring stress over shear rate. The slope of the linear regression was plotted as viscosity.

2.10. Quantifications

Quantification of cell viability (calceinAM/ethidium homodimer staining in mouse retinal dissociates and TUNEL staining in retinal organoid sections) was performed semi-automatically in Imaris version 8.3.1 using the spots analysis function. Quantification of rhodopsin and L/M opsin immunostaining expression, organoid size, brush border length, thickness of the outer nuclear layer (ONL) and inner nuclear layer (INL) were performed in Fiji. The average thickness of the ONL and INL was quantified from 10 different measurements in a whole tiled organoid section. Five measurements were averaged per organoid to obtain the average brush border height. The expression of L/M opsin and rhodopsin in thresholded images were normalized to the area of the ONL in each retinal organoid.

Quantification of the distribution of peripherin+ staining from the outer limiting membrane (OLM) was performed semi-automatically in Imaris version 10.0 using the spots analysis function to identify the peripherin+ areas. A surface was created of the retinal organoid to delineate the border of the OLM. A distance transformation was performed on the OLM surface, and the closest distance of each peripherin+ spot to the OLM boundary was plotted.

For scoring of TEM micrographs, each outer segment image was assessed by two scorers who were blinded to organoid treatment. Photoreceptor outer segments were identified adjacent to the mitochondria rich inner segments. The score for each outer segment was averaged and plotted on a histogram, normalized to the total number of outer segments analyzed for treatment and for control). A total of 108 outer segments from control (5 retinal organoids) and 88 outer segments from HA-treatment (5 retinal organoids) were analyzed.

2.11. Statistical methods

Statistical analysis was performed in Graphpad Prism version 9.1.1. A two-tailed *t*-test was performed to compare two groups and a one-way ANOVA with Turkey's post-hoc was performed for comparisons with more than two groups. For experiments with more than one independent variable, a two-way ANOVA with Sidak's post-hoc was performed. For data that was not normally distributed, non-parametric tests such as the Kruskal-Wallis (peripherin staining) and Mann-Whitney Wilcoxon test (outer segment scoring) were performed instead.

3. Results

3.1. Soluble HA improves mouse photoreceptor survival *in vitro*

Before testing the effects of HA in our human retinal organoid cultures, we first investigated the relationship between molar mass and cell survival. Given the greater ease of accessing mouse tissue, we cultured mouse retinal dissociates from postnatal day 3–5 C57BL/6 J mice in either retinal explant media (REM) or REM supplemented with 1 % HA (200 kDa). Cell viability was quantified using calceinAM and ethidium homodimer to stain live and dead cells, respectively. There was a significant increase in the number of viable cells at 3 and 5 d in culture (Fig. 1A and B). To quantify the number of live photoreceptors, the retinal cultures were dissociated, stained with CD73, and quantified by flow cytometry (Supplemental Fig. 1). Fluorescent counting beads were used to normalize between samples. Compared to the media control, there was a 4.3-fold and 2.8-fold increase in the number of live photoreceptors after HA treatment at 3 and 5 d *in vitro* (DIV), respectively (Fig. 1C).

The pro-survival effects of HA were also evident in cultures of FACS-purified photoreceptors (Fig. 1D and E). To determine if the pro-survival effect was dependent on the molar mass (MM) of HA, we examined a range from 20 to 1000 kDa, on FAC-sorted photoreceptor cultures. There was a significant increase in the percentage of live (calceinAM+) photoreceptors of all the HA treatments regardless of the MM used relative to the media control (Fig. 1F). Since the low, moderate, and high molar mass HA formulations were able to significantly enhance photoreceptor viability, we chose to continue to investigate the effects of the 200 kDa HA in human retinal organoid culture as it was easier to handle than higher molar mass HA.

3.2. HA supplementation impacts retinal organoid size, but not viability

Given that HA supported greater viability of mouse retinal dissociates, we wondered how exogenous HA would impact human retinal organoid growth and differentiation. Human retinal organoids express CD44, a known receptor for HA, which was confirmed by gene and protein expression (Supplemental Fig. 2). We hypothesized that the addition of the HA interphotoreceptor matrix component would improve retinal organoid lamination and enhance photoreceptor survival, thereby overcoming the necrotic core and disorganized inner layers that are common with the long culture periods of retinal organoids.

We quantified the size of the retinal organoids over time from brightfield images, which were normalized to the starting size of each organoid at week 14, prior to treatment (Fig. 2A and B). Interestingly, organoids grown in standard media conditions grew significantly larger, up to 70 % by week 26 (1.7 ± 0.4-times) compared to organoids cultured with HA, which remained consistent,

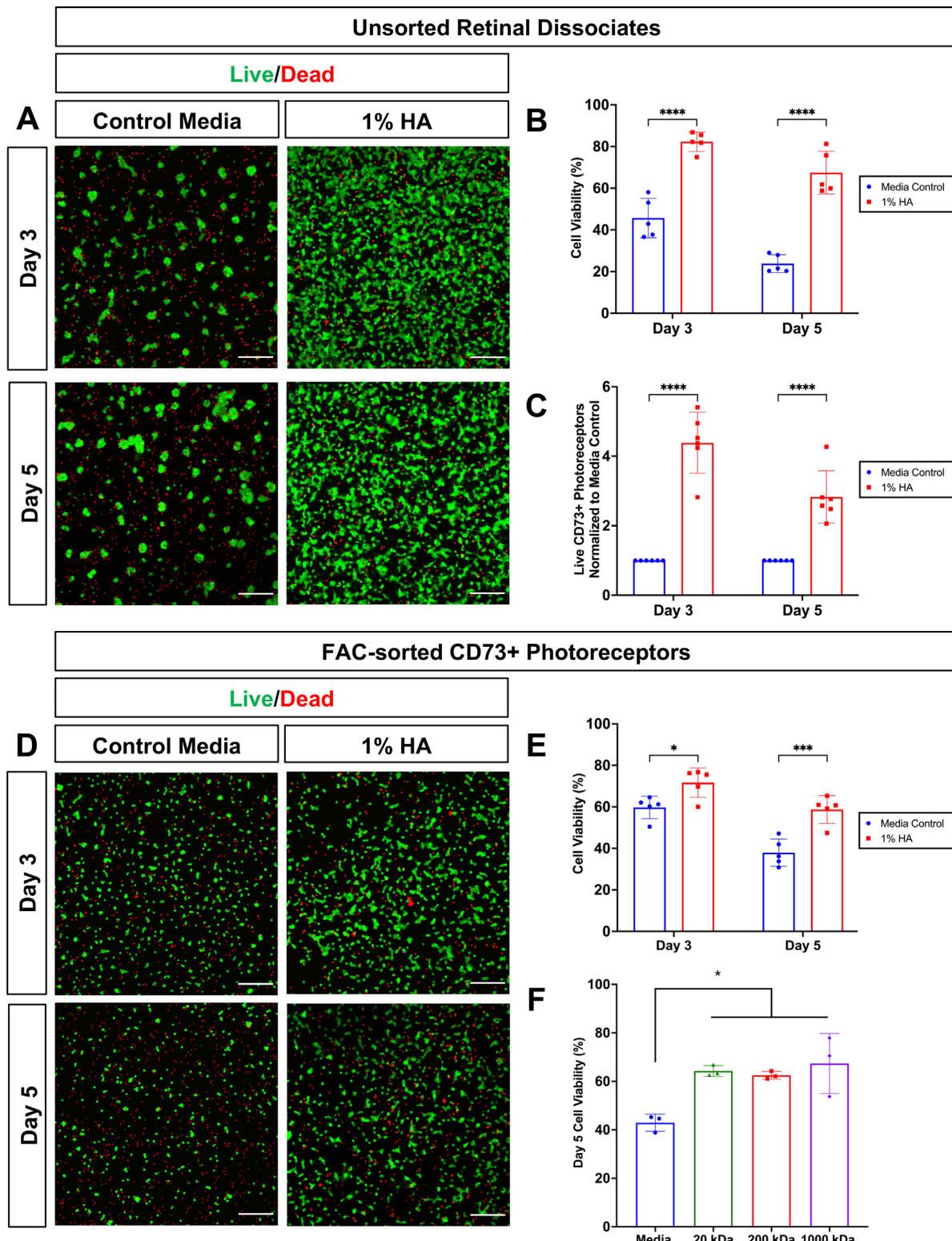


Fig. 1. Exogenous hyaluronan improves mouse photoreceptor cell viability. Retinal dissociates from P3-P5 wild type mice were cultured for 3 and 5 d in standard media or media supplemented with 1 % HA (200 kDa). A. Live cells (green) were stained with calceinAM and dead cells (red) were labelled using ethidium homodimer. Scale bar = 100 μ m. B. Quantification of cell viability in retinal dissociates was calculated as a% live (calceinAM+) cells over total (live and dead) cells. Data presented as mean \pm SD ($n = 5$ biological replicates), analyzed by two-way ANOVA with Sidak's post-hoc. C. Quantification of live CD73+ photoreceptors in retinal dissociate culture normalized to control media. Retinal dissociates were collected on days 3 and 5 and stained with CD73-APC and eFluor780 fixable viability dye. Fluorescent counting beads were added to each sample before flow cytometry acquisition and cell counts were normalized to control media. Data presented as mean fold-change \pm SD ($n = 3$ biological replicates), analyzed by two-way ANOVA with Sidak's post-hoc. D. FAC-sorted photoreceptors (CD73+) were cultured in control media or 1 % HA (200 kDa) *in vitro*. Cultures were stained on day 3 and 5 with calceinAM and ethidium homodimer for live imaging. E. Viable photoreceptors were quantified by calculating the percentage of live (calceinAM+) cells. Data presented as mean \pm SD ($n = 5$ biological replicates) analyzed by two-way ANOVA with Sidak's post-hoc. F. Viability of purified photoreceptors after 5 d of culture with different molar masses of HA. Quantifications of cell viability with supplementation with different molar masses HA (at 1 % concentration) after 5 d of *in vitro* culture. Data presented as mean \pm SD ($n = 3$ biological replicates) analyzed by one-way ANOVA with Tukey's post-hoc. * $p < 0.05$ *** $p < 0.001$ **** $p < 0.0001$.

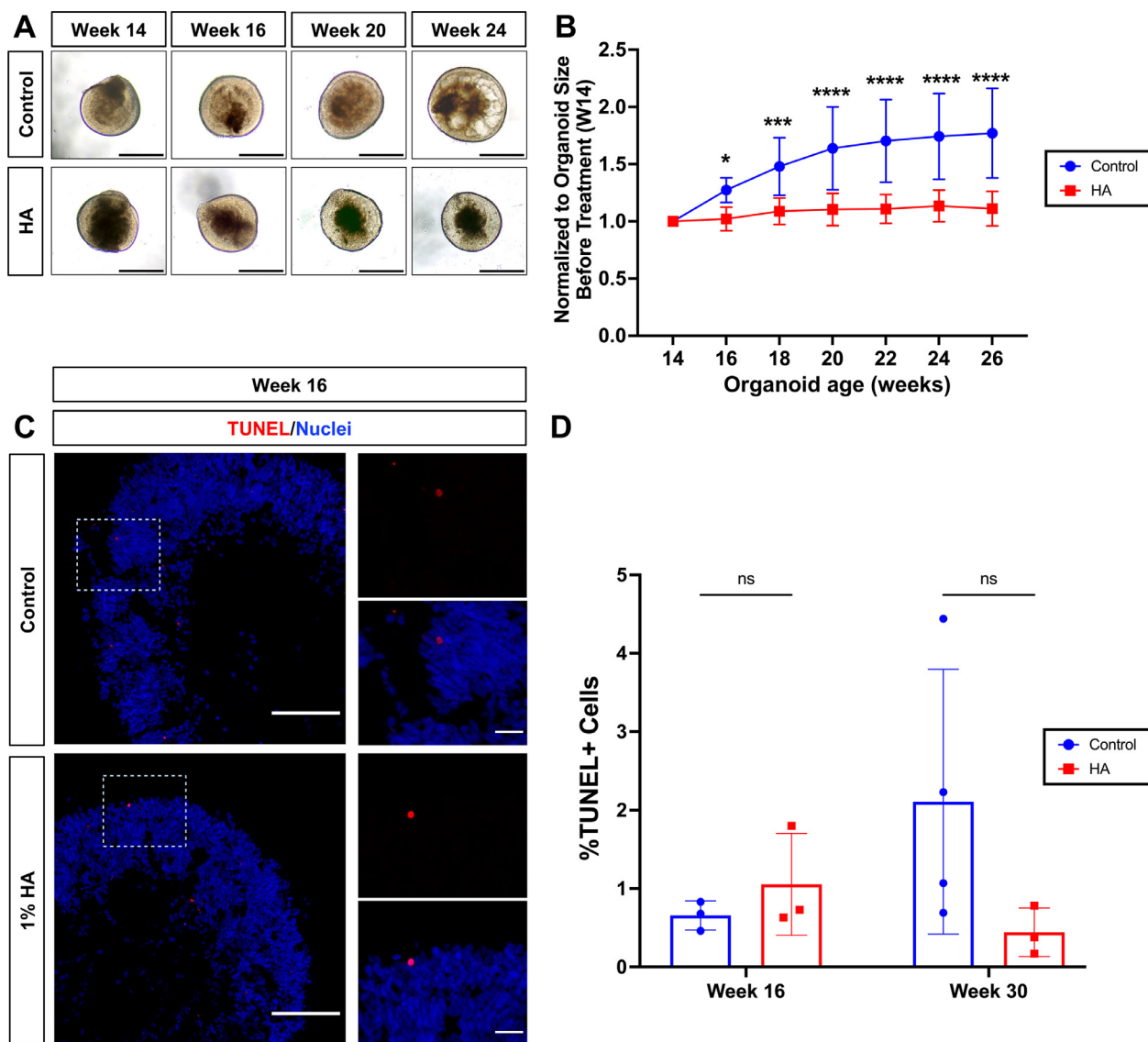


Fig. 2. HA supplementation maintains more uniform organoid sizes but does not impact their viability. A. Representative brightfield images of retinal organoids treated with 1 % HA over time. Scale = 500 μ m. B. Quantification of retinal organoid size over time normalized to pre-treatment size with or without the addition of HA. Data presented as mean \pm SD ($n = 10\text{--}14$ organoids from 2 independent differentiations) analyzed by two-way repeated measures ANOVA with Sidak's post-hoc, * $p < 0.05$, ** $p < 0.01$, *** $p < 0.001$, **** $p < 0.0001$. C. Representative images of TUNEL stained retinal organoids at week 16 (control and treated with 200 kDa HA). Scale bar = 100 μ m. Inset scale = 20 μ m. D. Quantification of TUNEL+ cells normalized to the total number of cells/organoid. Data presented as mean \pm SD ($n = 3\text{--}4$ organoids per timepoint).

with only a 10 % increase in size (1.1 ± 0.2 -times). Moreover, control retinal organoids were more variable in size compared to those treated with HA, as evidenced by larger standard deviations (39 % in control vs 15 % in HA). Thus, HA treatment produced smaller retinal organoids that appeared to be more consistent in size. HA-treatment impacted the overall size of retinal organoids over time after week 14, but not with treatment at week 8 (**Supplemental Fig. 3**). Thus, we chose to begin our HA supplementation with 1 % HA (200 kDa) from week 14 onward.

To investigate if the differences in organoid size were due to cell death, TUNEL staining was performed on retinal organoid sections (**Supplemental Fig. 4**). Interestingly, there were no significant differences in the number of TUNEL+ cells between HA-treated vs. media-control retinal organoids at week 16 or 30 (**Fig. 2C and D**). Moreover, dissociated retinal organoids from both groups had high cell viability as measured by trypan blue (**Supplemental Fig. 5**), indicating that changes in size after HA treatment are not due to differences in cell viability.

3.3. HA reduces RPC proliferation and accelerates photoreceptor commitment in human retinal organoids

Hyaluronan treatment maintained a consistent retinal organoid size, and thus, we wondered if this was due to differences in retinal progenitor cell (RPC) proliferation. Cone-rod homeobox (CRX), is a transcription factor that is expressed in committed post-mitotic rod and cone photoreceptors (**Fig. 3A and B** and (**Supplemental Fig. 6**). Using retinal organoids derived from the CRX-GFP H9 stem cell line, we quantified the proportion of photoreceptors (using a GFP reporter) and proliferating cells (Ki67+) through flow-cytometry (**Supplemental Fig. 7**). Week 16 ROs, which had been supplemented with HA for 2 weeks, had significantly fewer Ki67+ cells (15.6 ± 4.1 % HA-treated vs. 21.5 ± 4.0 % in control, $p = 0.0002$) and significantly more CRX-GFP+ photoreceptors (48.5 ± 4.8 % HA-treated vs 43.6 ± 4.1 % in control organoids, $p = 0.04$), suggesting that HA accelerated photoreceptor commitment (**Fig. 3C-E**). We also corroborated this result by quantifying

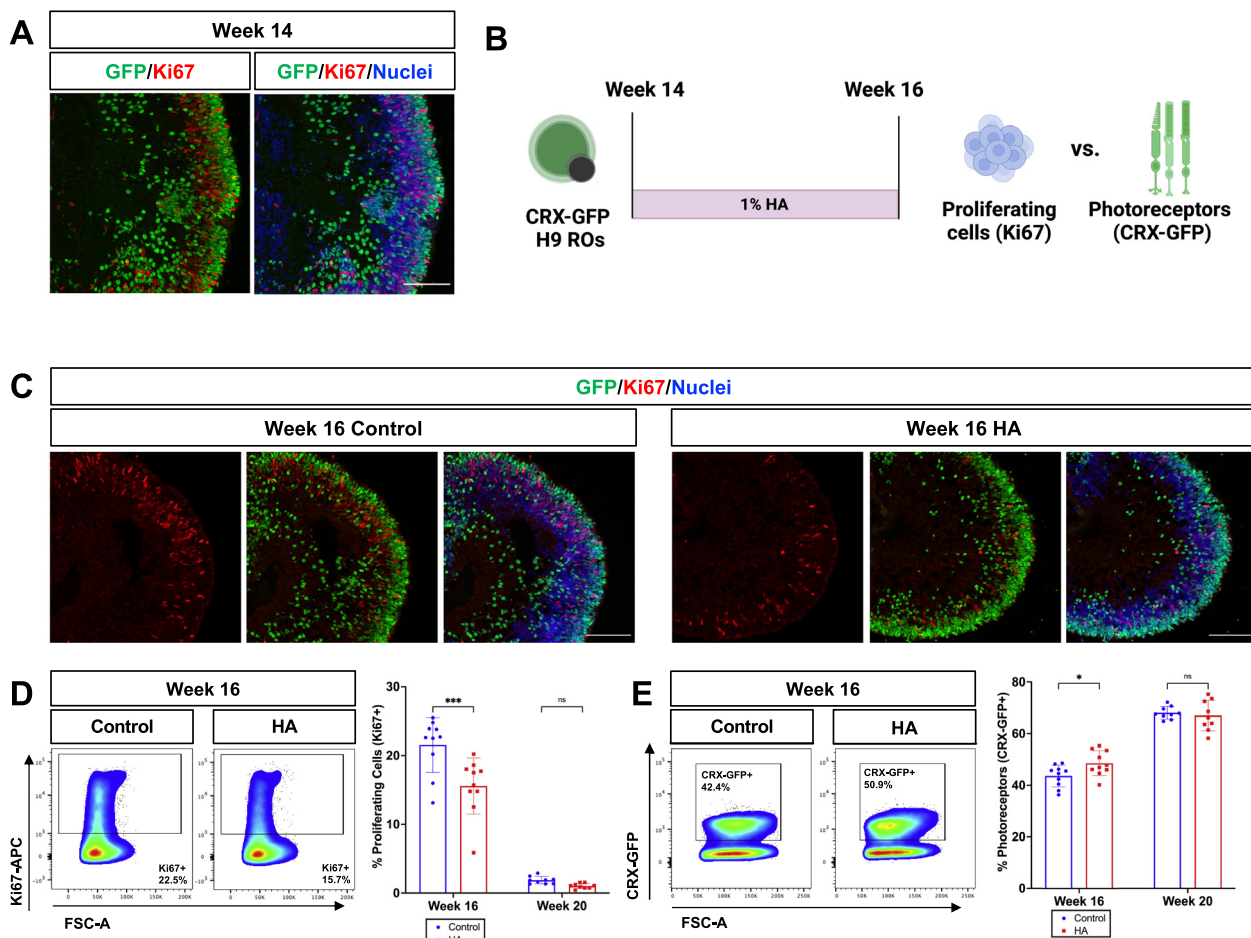


Fig. 3. Exogenous HA supplementation reduces cell proliferation and accelerates photoreceptor commitment in human retinal organoids. **A.** Representative week 14 retinal organoids stained for Ki67 (red), CRX-GFP (green), and Hoechst (nuclei, blue). Scale = 100 μ m. **B.** CRX-GFP H9-derived retinal organoids were treated with 1 % HA for two weeks. At week 16, organoids were harvested for flow cytometry to quantify the proportion of proliferating retinal progenitor cells (RPCs) with Ki67 and post-mitotic photoreceptors with CRX-GFP. **C.** Representative week 16 retinal organoid (treated with HA for two weeks and an aged-matched media control) stained with Ki67 and CRX-GFP. Scale bar = 100 μ m. **D.** Representative flow cytometry plot of dissociated retinal organoids gated for Ki67-APC and quantification of proliferating cells after 2 and 6 weeks of HA treatment using flow cytometry. **E.** Representative flow cytometry plot of dissociated retinal organoids gated for CRX-GFP and quantification of CRX-GFP+ photoreceptors after 2 and 6 weeks of HA treatment using flow cytometry. Data presented as mean \pm SD (n = 9-10 biological replicates from 3 independent differentiations) analyzed by two-way ANOVA with Sidak's post-hoc. * p < 0.05, *** p < 0.001.

recoverin expression at week 16 by flow cytometry: $39.4 \pm 5.9\%$ recoverin+ cells in HA vs. $30.6 \pm 3.7\%$ in age-matched, control organoids. (**Supplemental Fig. 8**). By week 20, there were no significant differences in the proportion of either proliferating cells or photoreceptors in the HA-treated vs. control organoids. This indicates that HA-supplementation did not produce more photoreceptors, but instead helped accelerate RPC differentiation into postmitotic CRX+ photoreceptors (**Fig. 3D** and **E**).

While we showed that HA molar mass did not impact mouse retinal cells, we wondered if it would affect human photoreceptor differentiation. We used flow cytometry to quantify Ki67 and CRX-GFP expression in retinal organoids treated at week 16 with either 20 or 200 kDa HA (Fig. 4A). Both significantly reduced proliferation and increased the proportion of photoreceptors compared to the media control, with a greater effect observed for the 200 kDa HA-treated group (Fig. 4B, and C). Thus, we continued using the 200 kDa HA to explore the effect of HA treatment on human retinal organoid differentiation.

3.4. HA treatment increases expression of photoreceptor-associated genes and preserves the Chx10+ inner nuclear layer

The increase in the proportion of CRX+ photoreceptors after 2 weeks of HA treatment led us to investigate other aspects of retinal

maturity. We looked at gene and protein expression at weeks 20 and 26 using qRT-PCR and immunohistochemistry (Fig. 5A). There was a significant upregulation of photoreceptor-associated genes in HA-treated ROs, including *RCVRN* (recoverin), *OPN1MW* (L/M opsin), *RHO* (rhodopsin) and *PRPH2* (peripherin-2), a gene encoding a protein involved in photoreceptor outer segment development, compared to media control samples (Fig. 5B). HA treatment did not affect expression of genes associated with bipolar cells, horizontal cells, or Müller glia (i.e., *PRKCa* (protein kinase c alpha), *CALB* (calbindin), and *GLUL* (glutamine synthetase)) (Fig. 5B). At 20 weeks, we observed downregulation in calbindin expression, which is expressed in horizontal cells; however, this was not significant by week 26 (Fig. 5B).

To see if changes in gene expression correlated with differences in retinal lamination, we examined retinal organoid sections to quantify the thickness of the outer nuclear layer (ONL), nuclei co-localizing with photoreceptor markers recoverin or rhodopsin, and the inner nuclear layer (INL), nuclei co-localizing with Chx10. While there were no significant differences in the thickness of the ONL, we observed a significantly thicker Chx10-positive INL in HA-treated organoids at week 26 (Fig. 5C and D). To better understand the effect of HA on the ONL, we examined rod and cone photoreceptors at weeks 20 and 26, measuring the pixel intensity of rhodopsin and L/M opsin expression, respectively, and

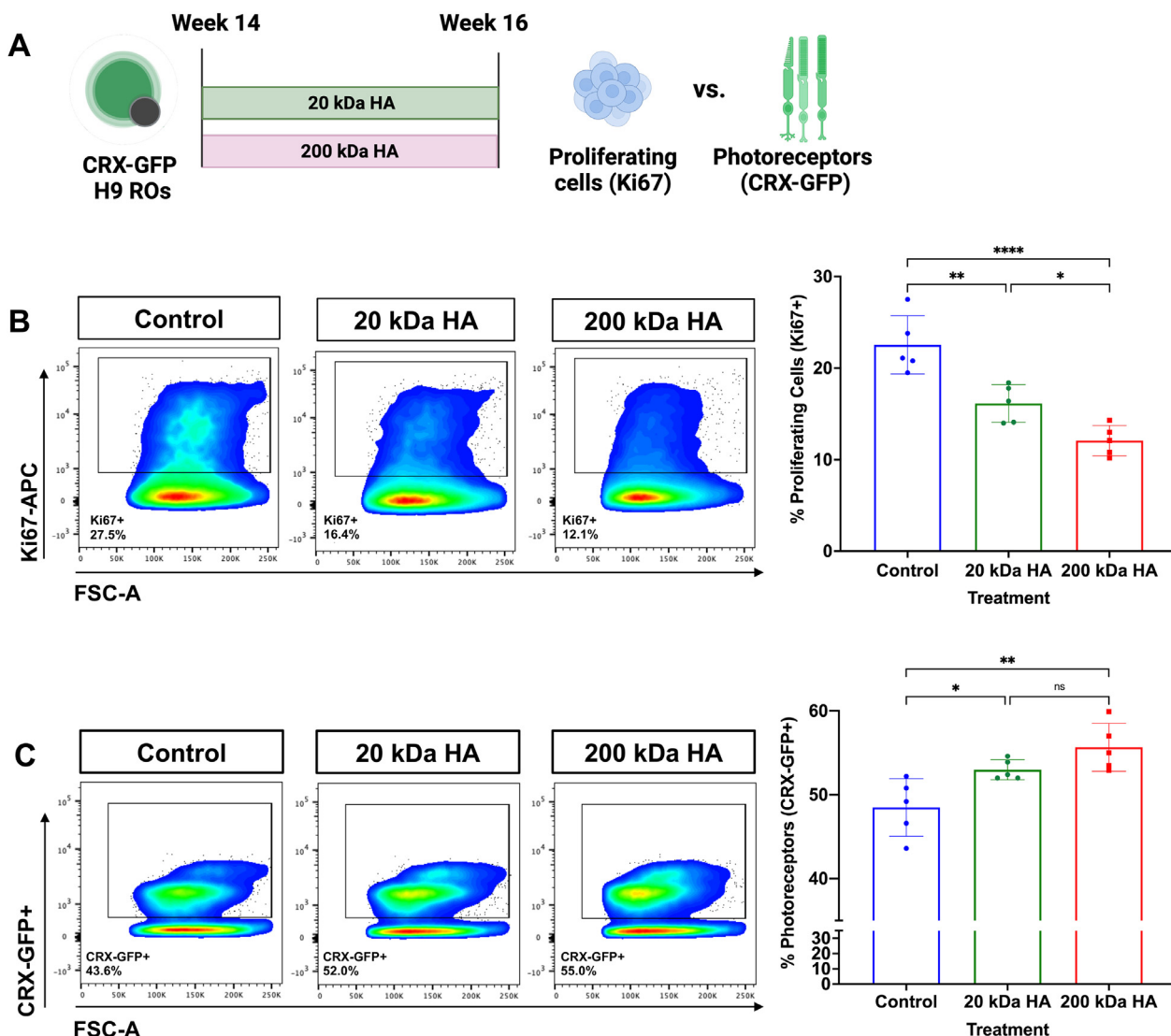


Fig. 4. HA molar mass affects the proliferative capacity and photoreceptor commitment in retinal organoids. A. Retinal organoids (CRX-GFP H9 derived) were supplemented with either 20 kDa or 200 kDa HA at 1 % concentration vs. media alone at 14 weeks of differentiation. After 2 weeks, the organoids were dissociated for analysis by flow cytometry. B. Quantification of Ki67+ cells and C. Quantification of CRX-GFP+ photoreceptors. Data presented as mean \pm SD ($n = 5$ biological replicates from 2 independent differentiations), analyzed by one-way ANOVA with Tukey's post-hoc. * $p < 0.05$, ** $p < 0.01$, **** $p < 0.0001$.

normalized to the area of the ONL. We observed significantly greater expression of rhodopsin staining in HA-treated organoids compared to controls at week 26 (Fig. 5E and F). Taken together, HA treatment in developing retinal organoids resulted in upregulation of photoreceptor-specific genes. While HA did not induce changes in the gene expression of cells in the inner retina, the integrity of the INL was likely better preserved due to regulation of cell proliferation and organoid size.

3.5. Brush border length and outer segments in human retinal organoids are shortened after HA treatment

We observed that HA increased the expression of photoreceptor-associated genes but were surprised by the reduced brush border layer length on the perimeter of the retinal organoids (Fig. 6A and B). The brush border layer is typically associated with photoreceptor maturation [6], and thus, shorter outer segments were initially concerning. At week 26, control retinal organoids had an average brush border layer of $32.0 \pm 6.7 \mu\text{m}$, which was significantly reduced with HA-treatment to $15.8 \pm 3.0 \mu\text{m}$ ($p = 0.0081$, Fig. 6C). We performed immunohistochemistry

on organoid sections to examine the brush border layer in more detail. This layer is composed of photoreceptor inner segments (IS) that are rich in mitochondria and peripherin+ outer segments (OS). It is demarcated by the outer limiting membrane (OLM) that forms the barrier between the outer nuclear layer (ONL), shown with phalloidin staining (Fig. 6D). Though the peripherin+ region was longer in control retinal organoids, the OS appeared to be more punctate and discontinuous compared to the thicker and more continuous peripherin staining in the HA-treated retinal organoids (Fig. 6D). The IS and OLM did not appear to be different between control and HA-treated retinal organoids, indicating that the OS that contributed to the differences in brush border length. The distance of peripherin+ outer segments from the OLM was significantly higher in the control retinal organoids compared to HA-treated organoids, and this was consistent across three different independent batches (Fig. 6E). Taken together, this suggests that there are structural differences in the photoreceptor outer segments after HA-treatment.

To better understand whether HA-treatment either prevented OS formation or led to its shrinkage, we delayed the addition of HA until after the brush border formed, starting at week 28

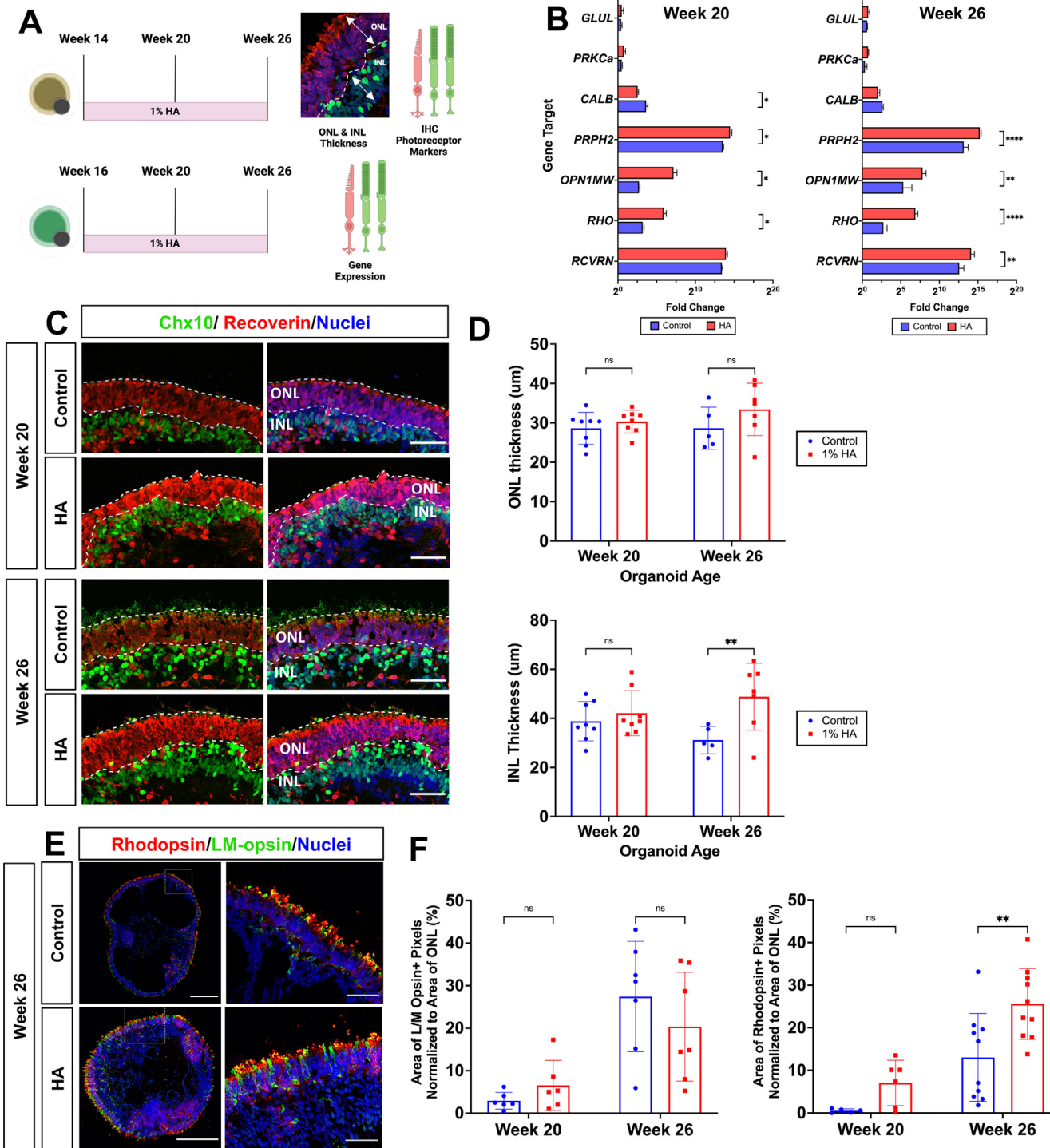


Fig. 5. Hyaluronan supplementation increases expression of photoreceptor genes and preserves retinal lamination. A. Retinal organoids were treated with 1% HA (200 kDa). Samples were collected at weeks 20 and 26 for qRT-PCR and immunohistochemistry to investigate retinal layer integrity and expression of photoreceptor-specific markers. B. Quantitative RT-PCR (qRT-PCR) of photoreceptor genes (*RCVRN*, *OPN1MW*, *RHO*, *PRPH2*), horizontal cells (*CALB*), bipolar cells (*PRKCa*), and Müller Glia (*GLUL*), in CRX-GFP retinal organoids treated from week 16 to weeks 20 and 26. Data presented as mean \pm SD ($n = 3$ biological replicates), analyzed by two-way ANOVA with Sidak's post-hoc. C. Representative images of HA-treated and age-matched control H9 retinal organoids (HA treatment initiated at week 14) stained with recoverin to denote the photoreceptors in the ONL and Chx10 to denote bipolar cells in the INL. The dashed white line denotes the border between the ONL and INL. D. Quantification of average ONL thickness in HA-treated retinal organoids (red) and age-matched controls (blue) by measuring the length of recoverin+ or rhodopsin+ nuclei and quantification of the average INL thickness by measuring the length of the Chx10+ nuclear layer. Scale bar = 50 μ m. Data presented as mean \pm SD ($n = 5-8$ retinal organoids from 2 independent differentiations), analyzed two-way ANOVA with Sidak's post-hoc, * $p < 0.05$. E. Representative images of week 26 H9 retinal organoids stained for L/M opsin (green), rhodopsin (red) and Hoechst (nuclei, blue) protein quantified by pixel intensity and normalized to the area of the ONL. Data presented as mean \pm SD ($n = 5-10$ retinal organoids from 2 to 3 independent differentiations), analyzed by two-way ANOVA with Sidak's post-hoc, ** $p < 0.01$.

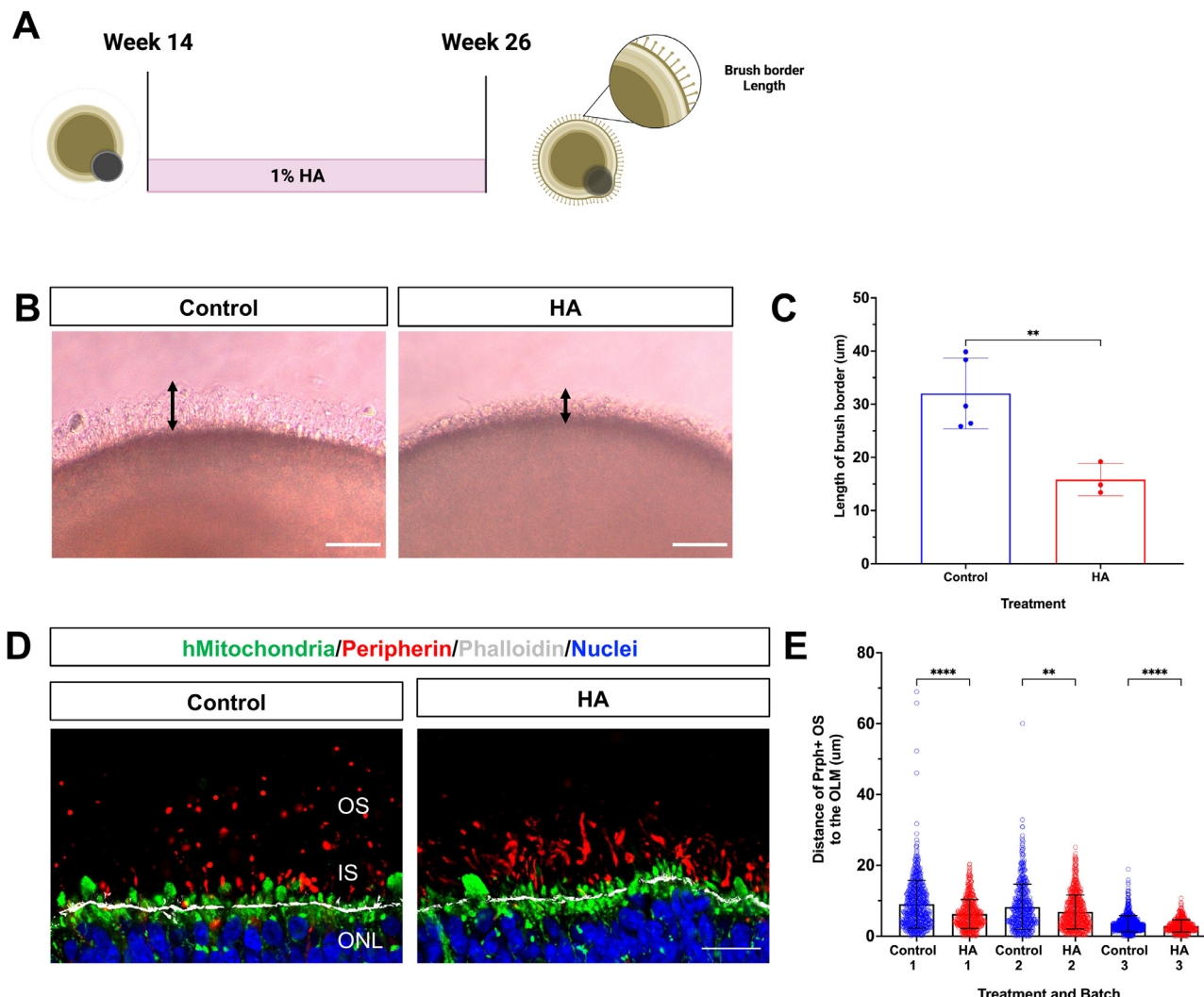


Fig. 6. Sustained hyaluronan supplementation reduces brush border length. A. Retinal organoids were treated with 1 % HA from weeks 14 to 26. B. Representative brightfield images with the dash line denote the edge of the brush border layer. Scale bar = 50 μm . C. Quantification of the brush border length (example denoted by the double-headed arrows). Data presented as mean \pm SD ($n = 3$ –5 organoids) analyzed by unpaired *t*-test, ** $p < 0.01$. D. Immunohistochemistry of photoreceptor inner segments (human mitochondria, green), outer segments (peripherin, red), OLM (phalloidin, white) and nuclei (Hoechst, blue). Scale bar = 20 μm . E. Quantification of the closest distance of peripherin+ outer segments to the OLM (mean \pm SD), sampled from 3 organoids per group in three independent differentiations, analyzed by Kruskal-Wallis test. ** $p < 0.01$, **** $p < 0.0001$.

instead of week 14, and quantified the length of the brush border 4 weeks later, at week 32 (Fig. 7A, **Supplemental Fig. 9**). The average brush border length started at approximately 41 μm at week 28: $41.2 \pm 3.2 \mu\text{m}$ for media controls and $40.7 \pm 7.8 \mu\text{m}$ for the HA-treated group. After 4 weeks of culture, the brush border layer increased to $61.7 \pm 9.8 \mu\text{m}$ in media control organoids whereas it decreased significantly to $29.0 \pm 1.6 \mu\text{m}$ with HA-treatment. The addition of HA to the media resulted in decreased photoreceptor outer segment length regardless if HA supplementation occurred before or after OS development (Fig. 7B-D). We used transmission electron microscopy (TEM) for ultrastructural analysis to further investigate OS-specific changes caused by the addition of HA (**Supplemental Fig. 10**). The IS regions were identified by their closer proximity to the OLM and their density of mitochondria. Representative TEM micrographs showed that, compared with age-matched controls, the HA-treated retinal organoids at week 32 (end of treatment period) had more organized disc structures with evidence of stacking within the OS regions (Fig. 7E). We performed unbiased, blinded scoring by 2 individuals of outer segments based on the formation and organization of disc structures, with scores ranging from 1 (no discs) to 6 (presence of organized disc struc-

tures, Fig. 7E). The distribution in the outer segment scores of retinal organoids treated with HA was significantly different from those of age-matched, controls by the Mann Whitney Wilcoxon Test (Fig. 7F). In the HA-treated retinal organoids, 17 % of outer segments were scored in the top 50th percentile (scores above 3), compared to 7.4 % from the age-matched controls (Fig. 7G). The shift in the distribution of organized disc structures in outer segments demonstrates that HA enhanced photoreceptor maturation.

3.6. Hyaluronan molar mass influences changes in the development of the brush border

We wondered if changes in the viscosity of HA-supplemented media would impact retinal organoid OS length. To answer this question, we examined the brush border length after 2 weeks of HA-treatment, using a series of HA molar masses (all at 1 % concentration, w/v), ranging from 20 to 1000 kDa (Fig. 8A and B). A rheometer was used to measure stress (Pa) over shear rate (1/s) (Fig. 8C), and viscosity was calculated from the slope of the linear regression (Pa \cdot s). The viscosity of the 20 kDa HA-supplemented media ($0.34 \pm 0.02 \times 10^{-3}$ Pa \cdot s) was simi-

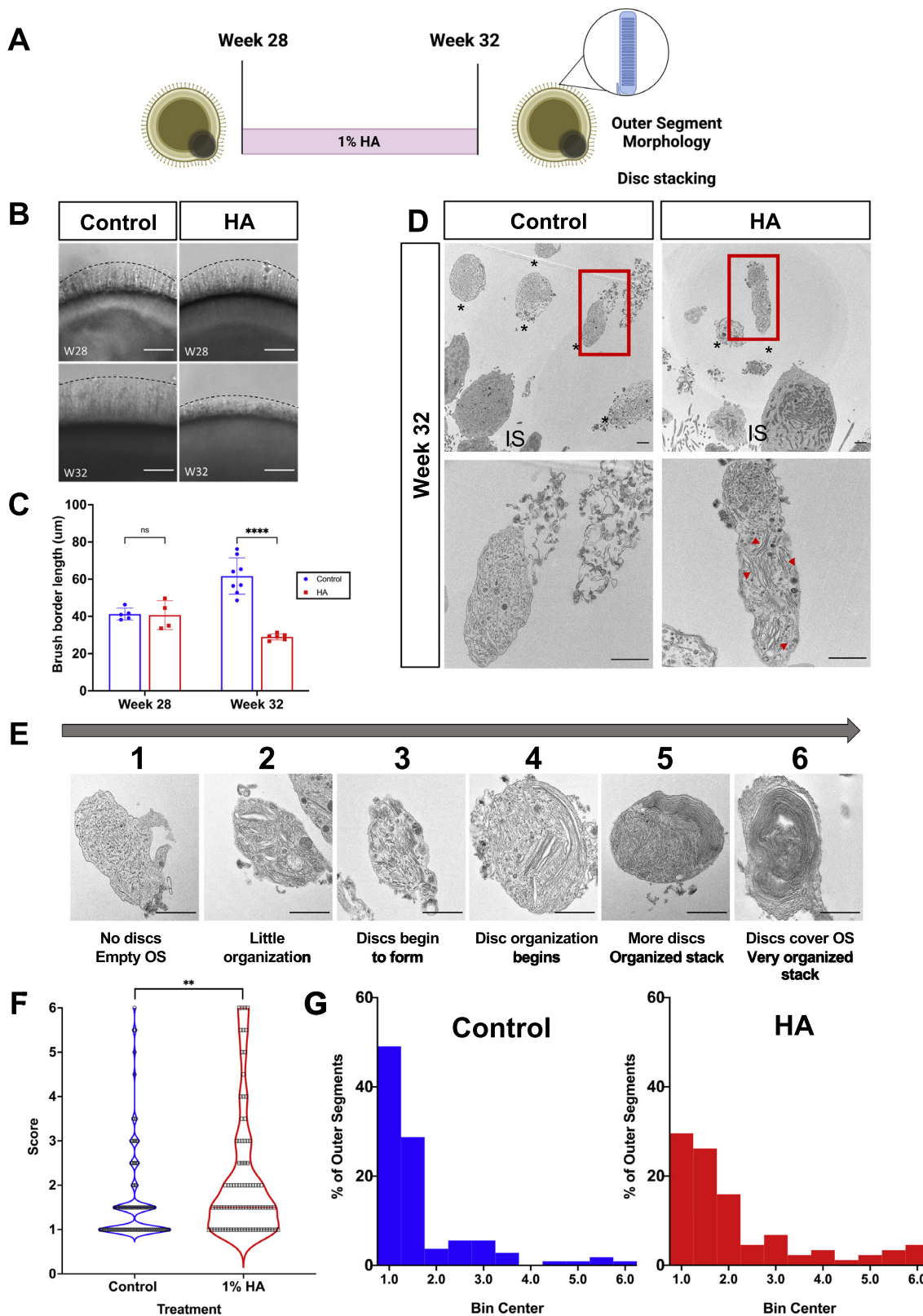


Fig. 7. Hyaluronan treatment after photoreceptor differentiation decreases brush border length and leads to enhanced disc formation. A. After 28 weeks of differentiation, retinal organoids were treated with either HA-supplemented media or media alone for an additional 4 weeks. B. Representative brightfield images of retinal organoids before (28 weeks) and after HA-treatment (32 weeks) relative to controls. Scale bar = 50 μ m. C. Brush border quantifications ($n = 4-8$ retinal organoids), analyzed using two-way ANOVA with Sidak's post-hoc. *** $p < 0.0001$. D. TEM micrographs of sectioned retinal organoids after 4 weeks of HA treatment. Asterisks denote outer segments (OS); IS is inner segment. Red arrows denote disc structures. Scale bar = 1 μ m. E. Outer segments were analyzed by 2 scorers who were blinded to the treatment on a scale based on formation and organization of stacked discs ranging from 1 (no disc formation) to 6 (organized disc structures), scale bar = 1 μ m. F. Violin plots showing the distribution of outer segment disc formation and organization for control and HA-treated retinal organoids ($n = 108$ outer segments imaged from 5 control retinal organoids, $n = 88$ outer segments imaged from 5 HA-treated retinal organoids). ** $p < 0.01$, analyzed by Mann Whitney Wilcoxon test. G. Histogram distribution plotting the percentage of outer segments in each bin for control (blue) and HA-treated (red) retinal organoids.

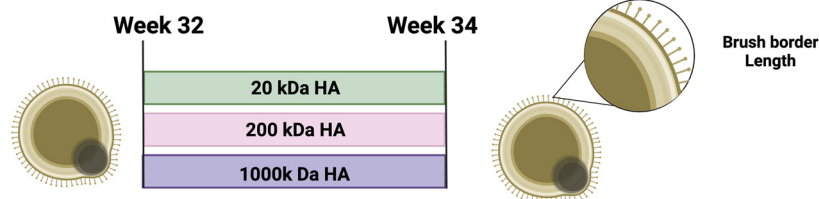
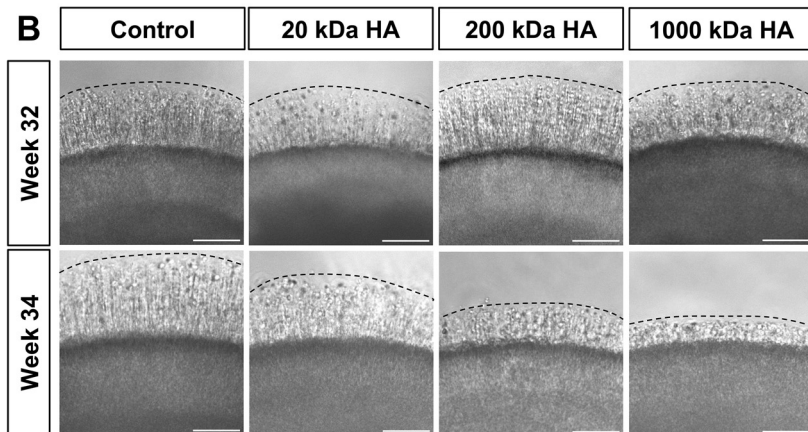
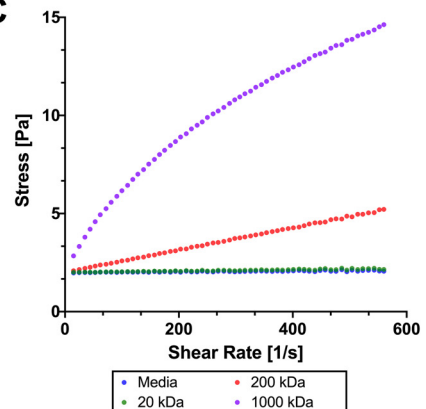
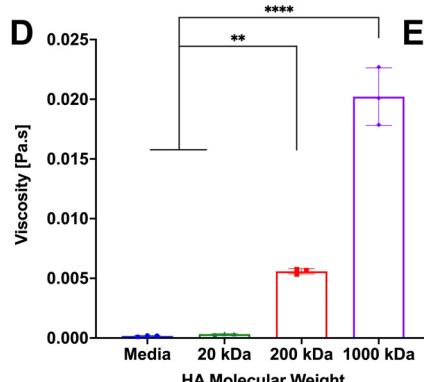
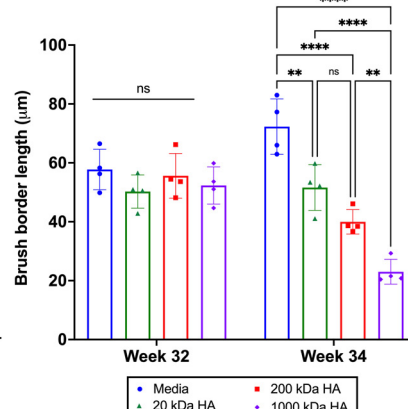
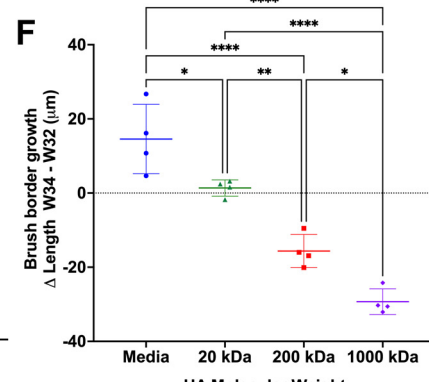
A**B****C****D****E****F**

Fig. 8. Reduction in brush border length is inversely related to the molar mass of hyaluronan. **A.** Retinal organoids were treated with 1 % HA from various molar mass polymers (ranging from 20 to 1000 kDa) from week 32 to week 34. **B.** Representative brightfield images of retinal organoids after 2 weeks of HA treatment, scale bar = 50 μ m. **C.** Representative rheology plot measuring stress [Pa] over shear rate [1/s] of media (control), 20 kDa, 200 kDa, and 1000 kDa HA-supplemented media. **D.** Viscosity, the slope of the linear fit of **C**, is plotted as Pa \cdot s, mean \pm SD ($n = 3$ measurements per sample), analyzed by one-way ANOVA with Tukey's post-hoc. **E.** Quantification of the brush-border length. Data presented as mean \pm SD ($n = 4$ organoids per treatment), analyzed by two-way ANOVA with Sidak's post-hoc. **F.** Quantification of brush border growth: week 34 minus baseline week 32 measurements, analyzed by one-way ANOVA with Tukey's post-hoc, * $p < 0.05$, ** $p < 0.01$, and *** $p < 0.0001$.

lar to that of the media control whereas all of the other molar masses of HA-supplemented media were significantly different (Fig. 8D): the 200 kDa ($5.6 \pm 0.25 \times 10^{-3}$ Pa \cdot s) and the 1000 kDa ($20.61 \pm 2.5 \times 10^{-3}$ Pa \cdot s) HA-supplemented media were both significantly more viscous than those of controls and 20 kDa. We measured the brush border length before and after the 2-week HA treatment. At 32 weeks of differentiation (pre-treatment), the average brush border length was approximately 54.0 ± 6.7 μ m. At 34 weeks, there were significant differences in brush border length between the media control versus all other formulations with HA-supplemented media (Fig. 8E). We compared the difference in brush border length at week 34 to that at week 32 for each organoid: the brush border of those organoids cultured in media alone grew an average of 14.6 ± 9.4 μ m whereas those cultured in HA either grew a negligible amount (20 kDa HA treated cultures grew by 1.4 ± 2.2 μ m) or shrunk: 200 kDa HA-treated ROs shrunk by an average of 15.6 ± 4.5 μ m and those with 1000 kDa by

29.3 ± 3.5 μ m (Fig. 8F). These results demonstrate that the reduction in the brush border length after 2 weeks of HA supplemented media is related to the viscosity of the growth media in which the organoids are cultured.

4. Discussion

Long-term maintenance of human stem cell-derived organoids remains a challenge in the field and has led to a series of adaptations to generate healthier retinal organoids for use in cell therapy and disease modelling. While all seven cell types of the retina can develop *in vitro*, the steadily increasing organoid size over time produces a nutrient gradient that cannot sustain the inner core, leading to necrosis and disappearance of the inner retinal layer before the photoreceptors can fully develop. Furthermore, while RPE secrete growth factors to support photoreceptor survival and development, its ectopic positioning does not properly recapitulate

the structural support provided by the native inner photoreceptor matrix (IPM). Thus, we aimed to improve the *in vitro* environment of differentiating retinal organoids through the addition of HA, as it is a major constituent of the IPM [30,31] and has been previously shown to enhance mouse photoreceptors viability *in vitro* [34].

While HA significantly increased the viability of dissociated mouse photoreceptors, it did not have any appreciable effects on the viability of whole retinal organoids, and the number of apoptotic TUNEL+ cells was quite modest even in intact control retinal organoids. While HA may have a prosurvival effect in dissociated cells, as other cell types in the intact retinal microenvironment may be contributing to the health of the intact organoid. Recent work by Völkner et al. characterized induced photoreceptor pathology by dual treatment with tumor necrosis factor and heparin-binding EGF-like growth factor in human retinal organoids and found insignificant differences in cell viability vs untreated controls [38]. They demonstrated that degenerating photoreceptors were extruded from the retinal organoids, which may also account for the lack of TUNEL+ cells in our treatment groups.

Human retinal organoids cultured in hyaluronan were smaller than the age-matched controls; however, this was not due to differences in cell death. These observations, combined with our flow cytometry data, suggest that hyaluronan promoted photoreceptor commitment, resulting in fewer proliferating Ki67+ RPCs. By week 20, the proportion of CRX+ photoreceptors between the HA-treated and age-matched controls was the same, which suggests that the majority of RPCs had differentiated into post-mitotic photoreceptors. This is consistent with the more modest increase in RCVRN gene expression compared to the significant upregulation in rod and cone opsin protein expression. The preserved Chx10+ inner retinal layer in our retinal organoids is most likely a consequence of the restricted organoid size, allowing for greater penetration of nutrients in the media. Genes associated with the inner retina were not significantly different (HA vs control) except for calbindin, expressed in horizontal cells, which was significantly downregulated at week 20 (after 4 weeks of HA treatment). The transient downregulation in calbindin expression may have been due to expedited RPC commitment into photoreceptors at the expense of horizontal cells, which are earlier born retinal neurons [39].

The findings from this study, based on our flow cytometry, gene expression and immunohistochemistry data, suggest that HA stimulates photoreceptor maturation. This effect is to be likely to be broadly applicable and can be further validated with retinal organoids derived from other hESC and iPSC derived cell lines. While we initially thought this would be associated with enhanced OS formation and thus a larger brush border layer, unexpectedly, HA-treated human retinal organoids had a brush border layer that was significantly smaller than age-matched controls. The development of the brush border layer, which forms above the outer limiting membrane in maturing retinal organoids, has been previously described by several groups [2,8,27,40] and has been associated with the development of the inner and outer segments. To provide better insight on the structural differences in a shorter brush border, we used confocal imaging to discriminate the inner and outer segments using human mitochondria and peripherin respectively. The peripherin staining in the control retinal organoids appeared to be more punctate and discontinuous, prompting us to examine outer segment morphology at the ultrastructural level by TEM. Photoreceptor outer segments are typically characterized by high membrane content from which discs evaginate and enclose upon maturation, a process mediated by actin polymerization [41–43]. The HA-treated organoids had a greater proportion of outer segments with stacked discs, which suggests that hyaluronan promoted photoreceptor maturation *in vitro*. West et al. reported

that the addition of antioxidants and BSA-bound fatty acids dramatically increased the disc packing and structure in human retinal organoids [27]. Our HA-treated human retinal organoids also had more outer segments with disc packing compared to age-matched media controls, albeit fewer than those observed physiologically. Defects in peripherin and trafficking of various opsin and membrane proteins to the outer segments have been associated with various forms of retinitis pigmentosa [44–46].

Mouse photoreceptor outer segments have been shown to range from 13 to 23 μm by ultrastructural analysis [47] whereas human inner/outer segment lengths have been reported at approximately 50 μm [48] using spectral-domain optical coherence tomography, which is comparable to our week 32 retinal organoids. Wahlin et al. reported that their retinal organoid outer segments reached a terminal length of approximately 39 μm [6]. Without HA treatment, the brush border layer in our retinal organoids continued to grow. Interestingly, regardless of organoid age, there was a significant reduction in the brush border length of our HA-supplemented cultures. We observed that the length of the brush border layer correlated inversely with the increased molar mass and viscosity of the HA-treated media: the highest molar mass HA (1000 kDa) caused the greatest decrease in brush border length. Viscosity has been shown to play a role in cancer cell migration and extravasation through activation of actin-related networks [49]. Outer segment formation, which is also dependent on actin-remodeling [43], may be enhanced by addition of these physical cues. Interestingly, the 20 kDa HA, which is not significantly different from media in terms of viscosity, also influenced the size of the brush border, with an increase of 1.3 μm after 2 weeks in HA compared to a 14 μm increase in media controls, which suggests that the effect of HA is not solely attributed to viscosity. In addition, there was reduced RPC proliferation and increased proportion of CRX+ photoreceptors to both 20 kDa and 200 kDa HA compared to the media controls. It is likely that controlling the viscosity by altering the concentration of HA would also produce differential effects on the brush border length. Future studies should explore the effect of timing, duration, and concentration of HA to influence photoreceptor development *in vitro*.

Others have investigated the effect of different polymers and peptides on retinal organogenesis [26,50]. Hunt et al. encapsulated human embryoid bodies (EBs) in HA, HA-gelatin, or RGD-alginate hydrogels from days 12 to 45 of retinal organoid differentiation [50]. Enhanced RPE and optic vesicle formation only occurred in the RGD-alginate hydrogels, and no significant effects were seen in conditions including HA. CD44, the receptor for HA, has been reported to be expressed in human retinal organoids around day 90 [36]. Functional blocking of CD44 in human retinal organoids reduced the number of rod photoreceptors and thinned the neuroepithelial layer, where the photoreceptors reside in the organoid, demonstrating that CD44 is required for retinal development. It is possible that day 12 EBs may not have had the appropriate HA receptors, as the hydrogel encapsulations in that study were performed at much earlier stages than our HA-treatment at week 14 (day 98). Changes in organoid size were not significant in retinal organoids treated with HA from week 8 (day 56) to week 10 (day 70), which is consistent with what was reported by Hunt et al.

Much of our investigations focused on the apical side of the retinal organoids and the development of outer segments, and not the axon terminals of the photoreceptors or other retinal cell types. Other studies have reported increased expression of synaptic proteins in retinal organoids cultured with decellularized ECM extracts [26]. Further investigations could focus on examining photoreceptor connectivity with the developing INL and whether HA supplementation *in vitro* correlates to improvements in their functional responsiveness to light using, for example, multielectrode arrays or calcium imaging [9,51]. Additional transcriptomic stud-

ies by scRNA-seq could offer more comprehensive insights on the changing dynamics as the increased proportion of differentiating photoreceptors could be at the expense of various retinal neurons, such as retinal ganglion cells, amacrine cells, or horizontal cells in differentiating HA-treated retinal organoids.

There is high variability in the proportion of retinal cell populations between differentiation methods, depending on the stem cell line, number of starting cells per well to form EBs, quick aggregation vs. slow gravity aggregation, the specific composition of exogenous factors, and the timing in which they are added to the differentiation media. Retinal organoid size varies tremendously, even within the same starting batch. Afanasyeva et al. and Döpper et al. have reported organoid sizes up to 1–1.5 mm, which is consistent with the range of our retinal organoids [40,52]. Many protocols have added BMP4 at the start of the differentiation, during EB formation, to promote optic vesicle formation [2,53], though its efficacy has been shown to be dependent on the iPSC cell line [54]. The use of basement membrane extracts such as Geltrex or Matrigel can also cause differential results in the efficiency of retinal organoid differentiations due lot-to-lot variability. The development of chemically defined hyaluronan-based materials would likely improve consistency.

To further enhance retinal organoid generation and long-term culture, hyaluronan should be incorporated into new technologies, such as additive manufacturing. Fabricated microwells and scaffolds from agarose, polydimethylsiloxane (PDMS), and poly(glycerol-sebacate), have been developed to both address the variable size in generating embryoid bodies, and to support long-term retinal organoid growth [51,55,56]. Sun et al. developed a 3D-printed PDMS microwell platform for long-term differentiation and maintenance of stem-cell derived retinal organoids. This platform is xenofree, as it does not use Matrigel or FBS, and can support RPE and the various cell types of the neural retina [57]. The addition of HA to this system would likely further enhance photoreceptor maturation.

A variety of different strategies, including hydrogels, microfluidic devices, and bioreactors, have been tested to improve the efficiency of retinal organoid culture. Achberger et al. co-cultured retinal organoids on a monolayer of RPE cells in a microfluidic chip to introduce fluid flow [28]. Retinal organoids were embedded in Hystem, a commercially available hyaluronan-based crosslinked hydrogel, which was placed on top of the RPE cell layer [28]. The distance between the RPE cell layer and the lectin-stained segments of their organoids was approximately 5 µm. The extremely short outer segments may be due to either the stiffness of the crosslinked Hystem hydrogel or the fluid flow in their microfluidic chip, as other groups have also reported the disappearance of the brush border layer after retinal organoid culture in stirred bioreactors [58]. The rational design and incorporation of hyaluronan and other well-defined ECM components into microfluidic, hydrogel, and scaffold-based systems would further improve retinal organoid maturation and consistency. Our findings show that viscosity and molar mass play important roles in maintaining the structures of photoreceptor outer segments, an important consideration for the design of new scaffolds to support organoid culture.

We demonstrate that hyaluronan enhances photoreceptor commitment and differentiation in human retinal organoids, leading to well-developed outer segments and preserved retinal architecture. Retinal organoid culture has allowed us to explore the effect of different molar masses of HA and viscosity on segment length and formation, which was not previously possible to investigate in 2D dissociated mouse photoreceptor cultures. These results highlight the importance of HA in the culture media, to produce more physiologically similar retinal organoids for disease modeling and cell therapy and may be broadly applicable to other human organoid cultures.

Declaration of competing interest

The authors declare the following financial interests/personal relationships which may be considered as potential competing interests: KK, YU, HN, HN, and YH are employees at Rohto Pharmaceuticals. The authors have a filed a patent on the application of HA on retinal organoids.

CRediT authorship contribution statement

Kotoe Kawai: Data curation, Writing – original draft, Writing – review & editing, Formal analysis. **Margaret T. Ho:** Conceptualization, Data curation, Formal analysis, Investigation, Writing – original draft, Writing – review & editing, Methodology. **Yui Ueno:** Data curation, Writing – review & editing. **Dhana Abdo:** Data curation, Writing – review & editing. **Chang Xue:** Methodology, Writing – review & editing. **Hidenori Nonaka:** Formal analysis, Writing – review & editing. **Hiroyuki Nishida:** Formal analysis, Writing – review & editing. **Yoichi Honma:** Formal analysis, Writing – review & editing. **Valerie A. Wallace:** Methodology, Writing – review & editing. **Molly S. Shoichet:** Conceptualization, Formal analysis, Funding acquisition, Methodology, Supervision, Writing – original draft, Writing – review & editing.

Acknowledgments

The authors thank Dr. Lindsey Fiddes and Yan Chen from the University of Toronto Microscope Imaging Laboratory for their technical expertise with confocal imaging, EM sample preparation/sectioning, and TEM imaging. We thank Dr. Majlinda Lako (Newcastle, UK) for her gift of the CRX-GFP H9 cell line. **Biorender.com** was used to make the schematics throughout the paper. We thank members of the Shoichet lab for their thoughtful review of this manuscript. This work was supported by the Canada First Research Excellence Fund (CFREF) through Medicine by Design (to MSS and VAW), Rohto Pharmaceuticals (to MSS, KK, and YU), the Natural Sciences and Engineering Research Council (NSERC, Discovery and Herzberg to MSS; Vanier CGS to MTH) and the Canadian Institutes of Health Research (CIHR, Foundation, and Project grant to MSS).

Supplementary materials

Supplementary material associated with this article can be found, in the online version, at [doi:10.1016/j.actbio.2024.05.001](https://doi.org/10.1016/j.actbio.2024.05.001).

References

- [1] M. O'Hara-Wright, A. Gonzalez-Cordero, Retinal organoids: a window into human retinal development, *Development* 147 (2020) dev189746, doi:[10.1242/dev.189746](https://doi.org/10.1242/dev.189746).
- [2] E.E. Capowski, K. Samimi, S.J. Mayerl, M.J. Phillips, I. Pinilla, S.E. Howden, J. Saha, A.D. Jansen, K.L. Edwards, L.D. Jager, K. Barlow, R. Valiuga, Z. Erlichman, A. Hagstrom, D. Sinha, V.M. Sluch, X. Chamling, D.J. Zack, M.C. Skala, D.M. Gamm, Reproducibility and staging of 3D human retinal organoids across multiple pluripotent stem cell lines, *Development* 146 (2019) dev171686, doi:[10.1242/dev.171686](https://doi.org/10.1242/dev.171686).
- [3] T. Nakano, S. Ando, N. Takata, M. Kawada, K. Muguruma, K. Sekiguchi, K. Saito, S. Yonemura, M. Eiraku, Y. Sasai, Self-formation of optic cups and storable stratified neural retina from human ESCs, *Cell Stem Cell* 10 (2012) 771–785, doi:[10.1016/j.stem.2012.05.009](https://doi.org/10.1016/j.stem.2012.05.009).
- [4] X. Zhong, C. Gutierrez, T. Xue, C. Hampton, M.N. Vergara, L.-H. Cao, A. Peters, T.-S. Park, E.T. Zambidis, J.S. Meyer, D.M. Gamm, K.-W. Yau, M.V. Canto-Soler, Generation of three dimensional retinal tissue with functional photoreceptors from human iPSCs, *Nat. Commun.* 5 (2014) 4047, doi:[10.1038/ncomms5047](https://doi.org/10.1038/ncomms5047).
- [5] F. Regent, H.Y. Chen, R.A. Kelley, Z. Qu, A. Swaroop, T. Li, A simple and efficient method for generating human retinal organoids, *Mol. Vis.* 26 (2020) 97–105.
- [6] K.J. Wahlin, J.A. Maruotti, S.R. Sripathi, J. Ball, J.M. Angueyra, C. Kim, R. Grebe, W. Li, B.W. Jones, D.J. Zack, Photoreceptor outer segment-like structures in long-term 3d retinas from human pluripotent stem cells, *Sci. Rep.* 7 (2017) 766, doi:[10.1038/s41598-017-00774-9](https://doi.org/10.1038/s41598-017-00774-9).

- [7] C.B. Mellough, J. Collin, M. Khazim, K. White, E. Sernagor, D.H.W. Steel, M. Lako, IGF-1 signaling plays an important role in the formation of three-dimensional laminated neural retina and other ocular structures from human embryonic stem cells, *Stem Cells* 33 (2015) 2416–2430, doi:10.1002/stem.2023.
- [8] A. Gonzalez-Cordero, K. Kruczak, A. Naeem, M. Fernando, M. Kloc, J. Ribeiro, D. Goh, Y. Duran, S.J.I. Blackford, L. Abelleira-Hervas, R.D. Sampson, I.O. Shum, M.J. Branch, P.J. Gardner, J.C. Sowden, J.W.B. Bainbridge, A.J. Smith, E.L. West, R.A. Pearson, R.R. Ali, Recapitulation of human retinal development from human pluripotent stem cells generates transplantable populations of cone photoreceptors, *Stem Cell Rep.* 9 (2017) 820–837, doi:10.1016/j.stemcr.2017.07.022.
- [9] S. Reichman, A. Slembrück, G. Gagliardi, A. Chaffiol, A. Terray, C. Nanteau, A. Potey, M. Belle, O. Rabesandratana, J. Duebel, G. Orieux, E.F. Nandrot, J.-A. Sahel, O. Goureau, Generation of storable retinal organoids and retinal pigmented epithelium from adherent human iPS cells in xeno-free and feeder-free conditions, *Stem Cells* 35 (2017) 1176–1188, doi:10.1002/stem.2586.
- [10] J. Collin, D. Zerti, R. Queen, T. Santos-Ferreira, R. Bauer, J. Coxhead, R. Hussain, D. Steel, C. Mellough, M. Ader, E. Sernagor, L. Armstrong, M. Lako, CRX expression in pluripotent stem cell-derived photoreceptors marks a transplantable subpopulation of early cones, *Stem Cells* 37 (2019) 609–622, doi:10.1002/stem.2974.
- [11] T. Zou, L. Gao, Y. Zeng, Q. Li, Y. Li, S. Chen, X. Hu, X. Chen, C. Fu, H. Xu, Z.Q. Yin, Organoid-derived C-KIT+/SSEA4+ human retinal progenitor cells promote a protective retinal microenvironment during transplantation in rodents, *Nat. Commun.* 10 (2019) 1205, doi:10.1038/s41467-019-10896-0.
- [12] G. Gagliardi, K. Ben MBarek, A. Chaffiol, A. Slembrück-Brec, J.-B. Conart, C. Nanteau, O. Rabesandratana, J.-A. Sahel, J. Duebel, G. Orieux, S. Reichman, O. Goureau, Characterization and transplantation of CD73-positive photoreceptors isolated from human iPSC-derived retinal organoids, *Stem Cell Rep.* 11 (2018) 665–680, doi:10.1016/j.stemcr.2018.07.005.
- [13] B. Dorgau, M. Georgiou, A. Chaudhary, M. Moya-Molina, J. Collin, R. Queen, G. Hilgen, T. Davey, P. Hewitt, M. Schmitt, S. Kustermann, F. Pognan, D.H. Steel, E. Sernagor, L. Armstrong, M. Lako, Human retinal organoids provide a suitable tool for toxicological investigations: a comprehensive validation using drugs and compounds affecting the retina, *Stem Cells Transl. Med.* 11 (2022) 159–177, doi:10.1093/sctfm/szab010.
- [14] K. Eade, S. Giles, S. Harkins-Perry, M. Friedlander, Toxicity screens in human retinal organoids for pharmaceutical discovery, *J. Vis. Exp.* (2021), doi:10.3791/62269.
- [15] M.N. Vergara, M. Flores-Bellver, S. Aparicio-Domingo, M. McNally, K.J. Wahlin, M.T. Saxena, J.S. Mumm, M.V. Canto-Soler, Three-dimensional automated reporter quantification (3D-ARQ) technology enables quantitative screening in retinal organoids, *Development* 144 (2017) 3698–3705, doi:10.1242/dev.146290.
- [16] K.-C. Huang, M.-L. Wang, S.-J. Chen, J.-C. Kuo, W.-J. Wang, P.N. Nhi Nguyen, K.J. Wahlin, J.-F. Lu, A.A. Tran, M. Shi, Y. Chien, A.A. Yarmishyn, P.-H. Tsai, T.-C. Yang, W.-N. Jane, C.-C. Chang, C.-H. Peng, T.M. Schlaeger, S.-H. Chiou, Morphological and molecular defects in human three-dimensional retinal organoid model of X-linked juvenile retinoschisis, *Stem Cell Rep.* 13 (2019) 906–923, doi:10.1016/j.stemcr.2019.09.010.
- [17] G. Li, G. Gao, P. Wang, X. Song, P. Xu, B. Xie, T. Zhou, G. Pan, F. Peng, Q. Zhang, J. Ge, X. Zhong, Generation and characterization of induced pluripotent stem cells and retinal organoids from a leber's congenital amaurosis patient with novel RPE65 mutations, *Front. Mol. Neurosci.* 12 (2019), doi:10.3389/fnmol.2019.00212.
- [18] M.-L. Gao, X.-L. Lei, F. Han, K.-W. He, S.-Q. Jin, Y.-Y. Zhang, Z.-B. Jin, Patient-specific retinal organoids recapitulate disease features of late-onset retinitis pigmentosa, *Front. Cell Dev. Biol.* 8 (2020), doi:10.3389/fcell.2020.00128.
- [19] D. Lukovic, A. Artero Castro, K.D. Kaya, D. Munezero, L. Gieser, C. Davó-Martínez, M. Corton, N. Cuenca, A. Swaroop, V. Ramamurthy, C. Ayuso, S. Erceg, Retinal organoids derived from hiPSCs of an AIPL1-LCA patient maintain cytoarchitecture despite reduced levels of mutant AIPL1, *Sci. Rep.* 10 (2020) 1–13, doi:10.1038/s41598-020-62047-2.
- [20] H. Xie, W. Zhang, M. Zhang, T. Akhtar, Y. Li, W. Yi, X. Sun, Z. Zuo, M. Wei, X. Fang, Z. Yao, K. Dong, S. Zhong, Q. Liu, Y. Shen, Q. Wu, X. Wang, H. Zhao, J. Bao, K. Qu, T. Xue, Chromatin accessibility analysis reveals regulatory dynamics of developing human retina and hiPSC-derived retinal organoids, *Sci. Adv.* 6 (2020), doi:10.1126/sciadv.aay5247.
- [21] C. Zheng, J.W. Schneider, J. Hsieh, Role of RB1 in human embryonic stem cell-derived retinal organoids, *Dev. Biol.* (2020), doi:10.1016/j.ydbio.2020.03.011.
- [22] W.-L. Deng, M.-L. Gao, X.-L. Lei, J.-N. Lv, H. Zhao, K.-W. He, X.-X. Xia, L.-Y. Li, Y.-C. Chen, Y.-P. Li, D. Pan, T. Xue, Z.-B. Jin, Gene correction reverses ciliopathy and photoreceptor loss in iPSC-derived retinal organoids from retinitis pigmentosa patients, *Stem Cell Rep.* 10 (2018) 1267–1281, doi:10.1016/j.stemcr.2018.02.003.
- [23] D.M. Gamm, E. Clark, E.E. Capowski, R. Singh, The role of FGF9 in the production of neural retina and RPE in a pluripotent stem cell model of early human retinal development, *Am. J. Ophthalmol.* 206 (2019) 113–131, doi:10.1016/j.ajo.2019.04.033.
- [24] Y. Guo, P. Wang, J.H. Ma, Z. Cui, Q. Yu, S. Liu, Y. Xue, D. Zhu, J. Cao, Z. Li, S. Tang, J. Chen, Modeling retinitis pigmentosa: retinal organoids generated from the iPSCs of a patient with the USH2A mutation show early developmental abnormalities, *Front. Cell Neurosci.* 13 (2019), doi:10.3389/fncel.2019.00361.
- [25] O. Strauss, The retinal pigment epithelium in visual function, *Physiol. Rev.* 85 (2005) 845–881, doi:10.1152/physrev.00021.2004.
- [26] B. Dorgau, M. Felemban, G. Hilgen, M. Kiening, D. Zerti, N.C. Hunt, M. Doherty, P. Whitfield, D. Hallam, K. White, Y. Ding, N. Krasnogor, J. Al-Aama, H.Z. Asfour, E. Sernagor, M. Lako, Decellularised extracellular matrix-derived peptides from neural retina and retinal pigment epithelium enhance the expression of synaptic markers and light responsiveness of human pluripotent stem cell derived retinal organoids, *Biomaterials* 199 (2019) 63–75, doi:10.1016/j.biomaterials.2019.01.028.
- [27] E.L. West, P. Majumder, A. Naeem, M. Fernando, M. O'Hara-Wright, E. Laning, M. Kloc, J. Ribeiro, P. Ovando-Roche, I.O. Shum, N. Jumbu, R. Sampson, M. Hayes, J.W.B. Bainbridge, A. Georgiadis, A.J. Smith, A. Gonzalez-Cordero, R.R. Ali, Antioxidant and lipid supplementation improve the development of photoreceptor outer segments in pluripotent stem cell-derived retinal organoids, *Stem Cell Rep.* (2022), doi:10.1016/j.stemcr.2022.02.019.
- [28] K. Achberger, C. Probst, J. Haderspeck, S. Bolz, J. Rogal, J. Chuchuy, M. Nikolova, V. Cora, L. Antkowiak, W. Haq, N. Shen, K. Schenke-Layland, M. Ueffing, S. Liebau, P. Loskill, Merging organoid and organ-on-a-chip technology to generate complex multi-layer tissue models in a human retina-on-a-chip platform, *Elife* 8 (2020), doi:10.7554/elife.46188.
- [29] A. Peters, L.S. Sherman, Diverse roles for hyaluronan and hyaluronan receptors in the developing and adult nervous system, *Int. J. Mol. Sci.* 21 (2020) 5988, doi:10.3390/ijms21175988.
- [30] J.G. Hollyfield, Hyaluronan and the functional organization of the interphotoreceptor matrix, *Invest. Ophthalmol. Vis. Sci.* 40 (1999) 2767–2769.
- [31] J.G. Hollyfield, M.E. Rayborn, M. Tammi, R. Tammi, Hyaluronan in the interphotoreceptor matrix of the eye: species differences in content, distribution, ligand binding and degradation, *Exp. Eye Res.* 66 (1998) 241–248, doi:10.1006/exer.1997.0422.
- [32] P. deS Senanayake, A. Calabro, K. Nishiyama, J.G. Hu, D. Bok, J.G. Hollyfield, Glycosaminoglycan synthesis and secretion by the retinal pigment epithelium: polarized delivery of hyaluronan from the apical surface, *J. Cell. Sci.* 114 (2001) 199–205, doi:10.1242/jcs.114.1.199.
- [33] Y. Inoue, M. Yoneda, O. Miyashita, M. Iwaki, M. Zako, Hyaluronan dynamics during retinal development, *Brain Res.* 1256 (2009) 55–60, doi:10.1016/j.brainres.2008.12.023.
- [34] N. Mitrousis, R.Y. Tam, A.E.G. Baker, D. van der Kooy, M.S. Shoichet, Hyaluronic acid-based hydrogels enable rod photoreceptor survival and maturation in vitro through activation of the mTOR pathway, *Adv. Funct. Mater.* 26 (2016) 1975–1985, doi:10.1002/adfm.201504024.
- [35] B.G. Ballios, M.J. Cooke, L. Donaldson, B.L.K. Coles, C.M. Morshead, D. van der Kooy, M.S. Shoichet, A hyaluronan-based injectable hydrogel improves the survival and integration of stem cell progeny following transplantation, *Stem Cell Rep.* 4 (2015) 1031–1045, doi:10.1016/j.stemcr.2015.04.008.
- [36] M. Felemban, B. Dorgau, N.C. Hunt, D. Hallam, D. Zerti, R. Bauer, Y. Ding, J. Collin, D. Steel, N. Krasnogor, J. Al-Aama, S. Lindsay, C. Mellough, M. Lako, Extracellular matrix component expression in human pluripotent stem cell-derived retinal organoids recapitulates retinogenesis in vivo and reveals an important role for IMPG1 and CD44 in the development of photoreceptors and interphotoreceptor matrix, *Acta Biomater.* 74 (2018) 207–221, doi:10.1016/j.actbio.2018.05.023.
- [37] M.A. Hayat, *Principles and Techniques of Electron Microscopy: Biological Applications*, Edward Arnold, 1981.
- [38] M. Völkner, F. Wagner, L.M. Steinheuer, M. Carido, T. Kurth, A. Yazbeck, J. Schor, S. Wieneke, L.J.A. Ebner, C. Del Toro Runzer, D. Taborsky, K. Zoschke, M. Vogt, S. Canzler, A. Hermann, S. Khattak, J. Hackermüller, M.O. Karl, HBEGF-TNF induce a complex outer retinal pathology with photoreceptor cell extrusion in human organoids, *Nat. Commun.* 13 (2022) 6183, doi:10.1038/s41467-022-33848-y.
- [39] E.A. Bassett, V.A. Wallace, Cell fate determination in the vertebrate retina, *Trends Neurosci.* 35 (2012) 565–573, doi:10.1016/j.tins.2012.05.004.
- [40] T.A. Afanasyeva, J.C. Corral-Serrano, A. Garanto, R. Roepman, M.E. Cheetham, R.W.J. Collin, A look into retinal organoids: methods, analytical techniques, and applications, *Cell. Mol. Life Sci.* (2021), doi:10.1007/s00018-021-03917-4.
- [41] T.R. Lewis, M.S. Makia, M. Kakakhel, M.R. Al-Ubaidi, V.Y. Arshavsky, M.I. Naash, Photoreceptor disc enclosure occurs in the absence of normal peripherin-2/rd5 oligomerization, *Front. Cell Neurosci.* 14 (2020) <https://www.frontiersin.org/articles/10.3389/fncel.2020.00092>. (accessed April 22, 2023).
- [42] R.Y. Salinas, J.N. Pearring, J.-D. Ding, W.J. Spencer, Y. Hao, V.Y. Arshavsky, Photoreceptor discs form through peripherin-dependent suppression of ciliary ectosome release, *J. Cell Biol.* 216 (2017) 1489–1499, doi:10.1083/jcb.201608081.
- [43] W.J. Spencer, T.R. Lewis, S. Phan, M.A. Cady, E.O. Serebrovskaya, N.F. Schneider, K.-Y. Kim, L.A. Cameron, N.P. Skiba, M.H. Ellisman, V.Y. Arshavsky, Photoreceptor disc membranes are formed through an Arp2/3-dependent lamellipodium-like mechanism, *Proc. Natl. Acad. Sci.* 116 (2019) 27043–27052, doi:10.1073/pnas.1913518117.
- [44] M. Kakakhel, L. Tebbe, M.S. Makia, S.M. Conley, D.M. Sherry, M.R. Al-Ubaidi, M.I. Naash, Syntaxin 3 is essential for photoreceptor outer segment protein trafficking and survival, *Proc. Natl. Acad. Sci.* 117 (2020) 20615–20624, doi:10.1073/pnas.2010751117.
- [45] S. Kohl, M. Christ-Adler, E. Apfelstedt-Sylla, U. Kellner, A. Eckstein, E. Zrenner, B. Wissinger, RDS/peripherin gene mutations are frequent causes of central retinal dystrophies, *J. Med. Genet.* 34 (1997) 620–626.
- [46] C.J.F. Boon, M.J. van Schooneveld, A.I. den Hollander, J.J.C. van Lith-Verhoeven, M.N. Zonneveld-Vrielink, T. Theelen, F.P.M. Cremer, C.B. Hoyng, B.J. Klevering, Mutations in the peripherin/RDS gene are an important cause of multifocal pattern dystrophy simulating STGD1/fundus flavimaculatus, *Br. J. Ophthalmol.* 91 (2007) 1504–1511, doi:10.1136/bjo.2007.115659.
- [47] L.D. Carter-Dawson, M.M. Lavail, Rods and cones in the mouse retina. I. Struc-

- tural analysis using light and electron microscopy, *J. Comp. Neurol.* 188 (1979) 245–262, doi:[10.1002/cne.901880204](https://doi.org/10.1002/cne.901880204).
- [48] G. Maden, A. Cakir, D. Icar, B. Erden, S. Bolukbasi, M. Elcioglu, The distribution of the photoreceptor outer segment length in a healthy population, *J. Ophthalmol.* 2017 (2017) e4641902, doi:[10.1155/2017/4641902](https://doi.org/10.1155/2017/4641902).
- [49] K. Bera, A. Kiepas, I. Godet, Y. Li, P. Mehta, B. Ifemembi, C.D. Paul, A. Sen, S.A. Serra, K. Stoletov, J. Tao, G. Shatkin, S.J. Lee, Y. Zhang, A. Boen, P. Mistriotis, D.M. Gilkes, J.D. Lewis, C.-M. Fan, A.P. Feinberg, M.A. Valverde, S.X. Sun, K. Konstantopoulos, Extracellular fluid viscosity enhances cell migration and cancer dissemination, *Nature* 611 (2022) 365–373, doi:[10.1038/s41586-022-05394-6](https://doi.org/10.1038/s41586-022-05394-6).
- [50] N.C. Hunt, D. Hallam, A. Karimi, C.B. Mellough, J. Chen, D.H.W. Steel, M. Lako, 3D culture of human pluripotent stem cells in RGD-alginate hydrogel improves retinal tissue development, *Acta Biomater.* 49 (2017) 329–343, doi:[10.1016/j.actbio.2016.11.016](https://doi.org/10.1016/j.actbio.2016.11.016).
- [51] C.S. Cowan, M. Renner, M. De Gennaro, B. Gross-Scherf, D. Goldblum, Y. Hou, M. Munz, T.M. Rodrigues, J. Krol, T. Szikra, R. Cuttat, A. Waldt, P. Papasaikas, R. Diggelmann, C.P. Patino-Alvarez, P. Galliker, S.E. Spirig, D. Pavlinic, N. Gerber-Hollbach, S. Schuierer, A. Srđanović, M. Balogh, R. Panero, A. Kusnyerik, A. Szabo, M.B. Stadler, S. Orgül, S. Picelli, P.W. Hasler, A. Hierlemann, H.P.N. Scholl, G. Roma, F. Nigsch, B. Roska, Cell types of the human retina and its organoids at single-cell resolution, *Cell* 182 (2020) 1623–1640 e34, doi:[10.1016/j.cell.2020.08.013](https://doi.org/10.1016/j.cell.2020.08.013).
- [52] H. Döpper, J. Menges, M. Bozeti, A. Brenzel, D. Lohmann, L. Steenpass, D. Kanber, Differentiation protocol for 3D retinal organoids, immunostaining and signal quantitation, *Curr. Protoc. Stem Cell Biol.* 55 (2020) e120, doi:[10.1002/cpsc.120](https://doi.org/10.1002/cpsc.120).
- [53] A. Kuwahara, C. Ozone, T. Nakano, K. Saito, M. Eiraku, Y. Sasai, Generation of a ciliary margin-like stem cell niche from self-organizing human retinal tissue, *Nat. Commun.* 6 (2015) 6286, doi:[10.1038/ncomms7286](https://doi.org/10.1038/ncomms7286).
- [54] V. Chichagova, G. Hilgen, A. Ghareeb, M. Georgiou, M. Carter, E. Sernagor, M. Lako, L. Armstrong, Human iPSC differentiation to retinal organoids in response to IGF1 and BMP4 activation is line- and method-dependent, *Stem Cells*, 2019, doi:[10.1002/stem.3116](https://doi.org/10.1002/stem.3116).
- [55] Y.H. Jung, M.J. Phillips, J. Lee, R. Xie, A.L. Ludwig, G. Chen, Q. Zheng, T.J. Kim, H. Zhang, P. Barney, J. Min, K. Barlow, S. Gong, D.M. Gamm, Z. Ma, 3D microstructured scaffolds to support photoreceptor polarization and maturation, *Adv. Mater.* 30 (2018) 1803550, doi:[10.1002/adma.201803550](https://doi.org/10.1002/adma.201803550).
- [56] I.-K. Lee, A.L. Ludwig, M.J. Phillips, J. Lee, R. Xie, B.S. Sajdak, L.D. Jager, S. Gong, D.M. Gamm, Z. Ma, Ultrathin micromolded 3D scaffolds for high-density photoreceptor layer reconstruction, *Sci. Adv.* 7 (2021) eabf0344, doi:[10.1126/sciadv.abf0344](https://doi.org/10.1126/sciadv.abf0344).
- [57] X. Sun, Z. Cui, Y. Liang, C. Duan, H.F. Chan, S. Mao, J. Gu, C. Ding, X. Yang, Q. Wang, S. Tang, J. Chen, One-stop assembly of adherent 3D retinal organoids from hiPSCs based on 3D-printed derived PDMS microwell platform, *Biofabrication* 15 (2023) 035005, doi:[10.1088/1758-5090/acc761](https://doi.org/10.1088/1758-5090/acc761).
- [58] P. Ovando-Roche, E.L. West, M.J. Branch, R.D. Sampson, M. Fernando, P. Munro, A. Georgiadis, M. Rizzi, M. Kloc, A. Naeem, J. Ribeiro, A.J. Smith, A. Gonzalez-Cordero, R.R. Ali, Use of bioreactors for culturing human retinal organoids improves photoreceptor yields, *Stem Cell Res. Ther.* 9 (2018), doi:[10.1186/s13287-018-0907-0](https://doi.org/10.1186/s13287-018-0907-0).